

Treatment of Linear and Nonlinear Dielectric Property of Molecular Monolayer and Submonolayer with Microscopic Dipole Lattice Model: I. Second Harmonic Generation and Sum-Frequency Generation

De-sheng Zheng[†], Yuan Wang[‡], An-an Liu[†], and Hong-fei Wang^{*}

*State Key Laboratory of Molecular Reaction Dynamics,
Institute of Chemistry, the Chinese Academy of Sciences, Beijing, China 100080*

(Dated: November 2, 2018)

Two crucial issues in the interface studies with the interface specific nonlinear spectroscopy are on how to describe the macroscopic dielectric constant of the molecularly thin layer and how to calculate the anisotropic two dimensional microscopic local field effect. In the currently accepted models of the nonlinear optics, the nonlinear radiation was treated as the result of an infinitesimally thin polarization sheet layer, and a three layer model was generally employed. The direct consequence of this approach is that an apriori dielectric constant, which still does not have a clear definition, has to be assigned to this polarization layer. Because the Second Harmonic Generation (SHG) and the Sum-Frequency Generation vibrational Spectroscopy (SFG-VS) have been proven as the sensitive probes for interfaces with the submonolayer coverage, the treatment based on the more realistic discrete induced dipole model needs to be developed. Here we show that following the molecular optics theory approach the SHG, as well as the SFG-VS, radiation from the monolayer or submonolayer at an interface can be rigorously treated as the radiation from an induced dipole lattice at the interface. In this approach, the introduction of the polarization sheet is no longer necessary. Therefore, the ambiguity of the unaccounted dielectric constant of the polarization layer is no longer an issue. Moreover, the anisotropic two dimensional microscopic local field factors can be explicitly expressed with the linear polarizability tensors of the interfacial molecules. Based on the planewise dipole sum rule in the molecular monolayer, crucial experimental tests of this microscopic treatment with SHG and SFG-VS are discussed. Many puzzles in the literature of surface SHG and SFG spectroscopy studies can also be understood or resolved in this framework. This new treatment may provide a solid basis for the quantitative analysis in the surface SHG and SFG studies.

I. INTRODUCTION

The past two and half decades have witnessed tremendous advancement and applications of the interface specific second order nonlinear optical techniques, mainly the surface second harmonic generation (SHG) and sum-frequency generation vibrational spectroscopy (SFG-VS), in molecular interface studies.^{1,2,3,4,5,6,7,8,9,10,11,12,13,14,15,16,17,18,19,20,21,22,23,24,25} To simply put it, SHG is the second order nonlinear process where two photons with the same fundamental frequency (ω) interact with a nonlinear medium simultaneously to generate a photon with the second harmonic frequency (2ω). If the two fundamental frequencies are not the same, a photon at the sum of these two frequencies can be generated from the so-called SFG process. Because of the symmetry requirement for the second order nonlinear processes, the leading dipolar term of the SHG or SFG processes is generally forbidden for the centrosymmetric bulk medium, and thus SHG and SFG become effective probes for the interface between the two centrosymmetric bulk phases.²⁶ The theoretical foundation and the experimental demonstration of the interfacial selectivity of SHG as well as SFG were pioneered by Shen and his colleagues since the early 1980's,^{27,28,29,30,31,32,33,34} extending from the original formulation of the light waves at the boundary of nonlinear media by Bloembergen *et al.* in the early 1960's.³⁵

With SHG and SFG-VS, equilibrium and dynamic behaviors of the molecular interface or film can be directly measured from the nonlinear electronic or vibrational spectroscopic response of the interfacial molecular moieties.^{2,6,8,10,11,24} One particular aspect of the studies in the past few years has been focused on the quantitative measurement and interpretation of the molecular orientation and vibrational spectra from the SHG and SFG-VS measurement on various molecular interfaces.^{21,25,36,37} Recent works also demonstrated that the coherent nature of the surface SHG and SFG-VS processes makes them more advantages over the other incoherent spectroscopic techniques used in surface studies. The interference of the molecular electric field and the strong polarization dependence in the SHG and SFG-VS response can be employed to investigate the detailed interactions and to determine the molecular conformation at the molecular interfaces.^{38,39,40}

However, researchers have long realized that the crucial issues in the quantitative interface studies with the SHG and SFG are on how to describe the macroscopic dielectric constant of the molecularly thin layer and how to calculate

[†] Also Graduate School of the Chinese Academy of Sciences.

[‡] An exchange graduate student at the Institute of Chemistry, the Chinese Academy of Sciences from the Department of Physics, Anhui Normal University, Wuhu, China 241000.

^{*} Author to whom correspondence should be addressed. E-mail: hongfei@iccas.ac.cn. Tel: 86-10-62555347. Fax: 86-10-62563167.

the anisotropic two dimensional microscopic local field effect.^{21,25,41,42,43,44,45,46,47,48,49,50,51,52,53} It has been well demonstrated that in majority cases the calculation of the molecular orientation is quite sensitive to the values used for these two factors.^{21,25,42,51,52}

In the currently accepted models of the nonlinear optics of interface,^{4,34,41,53,54,55} the nonlinear radiation was treated as the result of an infinitesimally thin polarization sheet layer, and as the starting point a macroscopic dielectric constant was assigned to this thin layer.^{4,34,54,55} This model was a natural extension of the original formulation by Bloembergen and Pershan, where a nonlinear plane parallel slab with a finite thickness embedded between two linear dielectrics was the source of the SHG radiation, and where the Maxwell's equations which satisfy the boundary conditions at the two plane interfaces were accurately solved.³⁵ However, according to that treatment, Bloembergen and Pershan concluded that the surface dipolar contribution to the SHG signal should be overwhelmed by the quadrupolar radiation in the much thicker boundary layer. Later experimental observations demonstrated that the surface dipolar contribution could be dominant in many cases. By solving the Maxwell's equations which satisfy the boundary conditions at the infinitesimally thin polarization sheet layer, Heinz and Shen provided the theoretical basis for the interface specific SHG, as well as the SFG-VS, in the interface studies.^{4,34,54,55}

Parallel to this macroscopic treatment, Ye and Shen employed a classical induced point-dipole model to include the microscopic local field effect on the nonlinear optical properties of adsorbed molecules on a substrate.⁵⁶ Shen later realized that from the theoretical point of view, the dielectric constant in the macroscopic model is not well defined for a monolayer because it is a macroscopic or mesoscopic property. Thus, Shen *et al.* tried to phenomenologically interpret this macroscopic dielectric constant as a result of the microscopic local field correction in a monolayer, and they also gave the explicit expressions for the macroscopic Fresnel factors and the microscopic local-field factors.^{41,53} Zhuang *et al.* also demonstrated that in a Langmuir monolayer it is satisfactory to treat the whole molecule with one unique microscopic local field factor derived from a modified Lorentz model of the interface.⁵³ This approach has been widely used for interpretation of the SHG and the SFG-VS data since.^{21,25}

However, puzzles and confusions remained in the SHG and SFG-VS practices on how the linear macroscopic dielectric constant and the microscopic local field factors, as described by Ye and Shen, should be used in the quantitative treatment of the experimental data. In their SHG measurement of the self-assembled-monolayer (SAM) at the gold substrate, Eisert *et al.* carefully compared the results with the macroscopic three layer model and the two layer model, as well as the local field corrections. They concluded that using the two-layer model without local-field correction gave most satisfactory agreement of the molecular orientation with the results from the NEXAFS and IR spectroscopy measurements.⁵¹ This work is obviously not consistent with the above treatment by Shen *et al.* It was further criticized by Roy on the inconsistency that the SAM film is considered anisotropic for SHG but assumed to be isotropic in terms of its linear optical properties.⁵⁷ Roy then outlined a macroscopic phenomenological model that treats linear and nonlinear optics of the anisotropic interface layer in a single framework, which nevertheless requires a minimum of six unknown parameters of the interfacial optical constants even for an uniaxial monolayer in SHG or SFG-VS.^{57,58} Thus, Roy concluded that the conventional SHG measurement of phase and intensity may not be enough to determine the orientation of SAM. However, even though the anisotropy is undoubtedly significant on the nonlinear responses, Roy's criticism might have exaggerated the influence of the anisotropy on the linear optical property within the monolayer, which in fact only slightly modifies the reflectivity of the surface as judged from ellipsometry measurement.^{26,59,60,61}

There have been a few experimental and empirical theory studies on the SHG data from the interfacial monolayer, using different parameters of the macroscopic three layer model plus the microscopic local field factors.^{43,44,45,46,47,48,49,50,51,62,63,64} In dealing with the macroscopic dielectric constant, generally one of the two bulk phase values were used, reducing the macroscopic problem to the same as the so-called two phase model.^{65,66} However, because the two phase model does not consider the different microscopic properties of the surface molecular layer, it can only phenomenologically describe the surface SHG process, and it generally fails to qualitatively explain the observed differences in the SHG measurement. On the other hand, in dealing with the microscopic local field factors, some works followed the classical dipole model as presented by Ye and Shen, and the rest followed the simple Lorentz-Lorenz local field expression using the bulk polarizabilities.^{63,64}

Another approach completely neglects the treatment of the microscopic local field effect, and treated the molecular film with a macroscopic three layer model.^{42,52,58,67,68,69,70,71} In SFG-VS, some considered the film anisotropic and its optical constant is determined using the Clausius-Mossotti relationship with the ellipsometry data of the film.⁷¹ This is obviously rooted in the practices of the ellipsometry studies, where it is generally believed that the macroscopic optical model can be valid down to the monolayer level.^{59,60} In SHG, some considered the film isotropic and the optical constant can be obtained from the Kramers-Kronig dispersion relationship measured from the bulk or thin film UV-Visible absorption spectra.^{42,69,70} When the molecule is considered with uniaxial symmetry, the ratio between the dielectric constants of the fundamental and the SH frequency can be directly determined from the intensity ratio in the polarization measurements.^{37,42} There are also efforts trying to show that the dielectric constant of the extremely thin monolayer is just the simple arithmetic average of the two bulk dielectric constants.^{52,58,67,68} Even though the results from these approaches seemed reasonable, neglecting the anisotropic microscopic local field effect in the molecular monolayer is not likely to be physically sound.

All the above approaches gave the similar trend in the variation of molecular orientation. However, the value of the

orientational angle depends quite significantly on the different parameters used. Besides all the different approaches in the SHG and SFG-VS data analysis, the experimental studies have shown that the initial treatment by Heinz and Shen with the infinitesimally thin polarization sheet layer is generally correct. Researchers in the field also agree that the definition of the dielectric constant of the monolayer or even submonolayer film is unclear and meaningless in the macroscopic optics, because when the film is as thin as one molecular layer the macroscopic reflection and transmission coefficients simply converge to the bare interface limit.^{58,59,60} Therefore, even though the treatment provided by Shen and coworkers is generally valid, there are still issues need to be clarified. One problem in the existing model is that the macroscopic and microscopic linear optical properties of the nonlinear molecular layer are not totally compatible. In practice we also need a more detailed microscopic theory to help understand the detailed SHG or SFG-VS responses from different molecular interface or film.

Aside from the above, a microscopic theory of molecular crystal surface SHG was proposed by Munn in the early 1990's.⁷² In this formulation, since the surface SHG response is treated microscopically as a sum of responses from successive surface layers, the introduction of a dielectric constant of the surface layer was not required, and this incidentally yielded a microscopic expression of the dielectric constant of the surface layer. Subsequent studies by Munn and coworkers used the planewise sum rules in the molecular crystal dielectric theory^{73,74,75,76,77,78} to simulate the linear and nonlinear optical responses of the model Langmuir-Blodgett films.^{49,79,80,81,82} In these treatment, Munn *et al.* concluded that improper treatment of the local fields can result in significant errors in determination of the molecular angle from the SHG data.^{79,80} They also showed that in order not to overestimate the microscopic local field factors for the closely packed monolayer films, the monolayer itself had to be segmented into several layers.^{49,82} In the microscopic theory, the microscopic local field factors depend on the orientation and distribution of the interfacial dipoles, and the microscopic local field factors are needed to determine the dipole orientation from the SHG data. Therefore, Pannhuis and Munn suggested that a self-consistent approach needs to be employed to solve the problem.⁸⁰ These microscopic theory and simulations certainly provided new insights on the treatment of the SHG from the molecular monolayer as well as multilayers. These insights may contain answers to the questions raised above. However, the implications of these works are yet to be picked up by the field.

Because the SHG and the SFG-VS have been proven as the sensitive probes for interfaces with the submonolayer coverage,^{2,4,8,10} the treatment based on the more realistic discrete induced dipole model needs to be developed. According to Born and Wolf, the molecular optics theory can directly connect the macroscopic optical phenomena to the molecular properties, and can provide deeper physical insight into electromagnetic interaction problems than does the rather formal approach based on Maxwell's phenomenological equations.^{83,84} From the above analysis, we realized that different from the infinitesimally thin polarization sheet layer model treated on the basis of the Maxwell theory, a molecular optics treatment can be developed to describe the coherent SHG or SFG-VS radiation from a discrete lattice in between the two isotropic phases. We shall show in this report that even though there is no general methods to solve the integro-differential equations of molecular optics, the summation, or integration, of the radiation in the far field from a discrete induced dipole lattice can be rigorously solved with the application of the principle of the stationary phase.⁸⁴

The discrete induced dipole lattice model is a more realistic description of the molecular interface than the infinitesimally thin polarization sheet layer model.⁸⁵ Because the SHG and the SFG-VS processes are known with interface selectivity, the whole problem of the integro-differential equations is greatly simplified since the summation over the second harmonic or sum-frequency radiation fields from the discrete interface induced dipoles needs to be calculated. According to the Ewald-Oseen extinction theorem in the molecular optics, there exists only the incident field in vacuum and the dipolar microscopic radiation field in vacuum emitting from each induced dipole.^{35,83,84} Since the whole problem is treated microscopically as radiation from the discrete induced dipoles, and the total radiation is calculated through summation, or integration, over the whole dipole lattice, there is no need to use the Maxwell equations together with the boundary conditions as in the infinitesimally thin polarization sheet layer model. This works because as Lalor and Wolf pointed out that the Ewald-Oseen extinction theorem just plays the role of the boundary condition.⁸³ Therefore, there is no need to use the boundary conditions, where a macroscopic dielectric constant has to be defined in order to apply the boundary conditions for a finite volume across the boundary area which includes the molecular monolayer. Therefore, the macroscopic dielectric constant for the molecular monolayer, which has difficulties to be defined in the previous treatment, is just a nuisance parameter in this microscopic, and it is finally able to be gotten rid of. There was a section in their classic paper where Bloembergen and Pershan,³⁵ showed that the approach using the integral equation based on the Ewald-Oseen extinction theorem reached exactly the same results for the nonlinear response from the nonlinear plate parallel slab.^{35,86} This certainly helps to justify the microscopic molecular optics approach to be employed.

In the next few sections, we shall show that the SHG radiation in the far field from the discrete dipole lattice is in the same form as from the infinitesimally thin polarization sheet layer model. Moreover, in this discrete induced dipole model, the introduction of the polarization sheet is no longer necessary, therefore, the ambiguity of the unaccounted dielectric constant of the polarization layer is no longer an issue. Incidentally, the anisotropic two dimensional microscopic local field factors can be explicitly expressed with the linear polarizability tensors of the interfacial molecules. Based on the planewise dipole sum rule in the molecular monolayer, crucial experimental tests of this treatment with the SHG and SFG-VS experiments are going to be discussed. We shall also discuss the puzzles in

the literature of the surface SHG and SFG spectroscopy studies as discussed above. This microscopic treatment can provide a solid basis for the quantitative analysis of the surface SHG and SFG studies.

II. THE INDUCED DIPOLE OF THE MONOLAYER WITH THE DISCRETE POINT-DIPOLE LATTICE MODEL

Because the SHG and the SFG-VS have been proven as the sensitive probes for interfaces with the submonolayer coverage,^{2,4,8,10} the treatment based on the more realistic discrete induced dipole model needs to be developed. Here we derive the expressions of the linear and nonlinear induced dipole of the monolayer with the discrete point-dipole lattice model. Some aspects of the discussions below can be found in the earlier paper by Ye and Shen.⁵⁶

In the classical molecular optics, the response of the medium to the incident field is described by means of the electric-dipole moments that are induced in the molecules of the medium under the action of the incident field.^{83,84} When an optical field at a frequency ω is incident on a medium, it creates induced dipole at the incident frequency and its higher harmonics in that medium through the total field that each dipole or molecule experiences. This total field is called the local field \vec{E}_{loc} . The higher harmonic induced dipole can be viewed as the results of multiple interactions with the local optical field. Therefore, they are only strong enough for detection when the optical field is intense enough. The induced dipole at the incident frequency is the source of the radiation in the linear processes, while the others are the source responsible for the radiation in the nonlinear processes. Simply to put it, one has

$$\vec{\mu}_{induced} = \vec{\mu}_{induced}^{linear} + \vec{\mu}_{induced}^{non-linear} \quad (1)$$

Nonlinear optics has been an extensively studied field since the invention of the first laser in the early 1960's.^{26,87} Here we only discuss the linear and the second harmonic process in an optical medium. Considering the fact that both fields in the linear frequency and the resulted second harmonic can contribute to the induced dipole at the second harmonic frequency, one has

$$\begin{aligned} \mu_i &= \mu_i^\omega + \mu_i^{2\omega} \\ &= (\alpha_{ix}^\omega \ \alpha_{iy}^\omega \ \alpha_{iz}^\omega) \begin{pmatrix} E_{loc,x}^\omega \\ E_{loc,y}^\omega \\ E_{loc,z}^\omega \end{pmatrix} \\ &\quad + (E_{loc,x}^\omega \ E_{loc,y}^\omega \ E_{loc,z}^\omega) \begin{pmatrix} \beta_{ixx} & \beta_{ixy} & \beta_{ixz} \\ \beta_{iyx} & \beta_{iyy} & \beta_{iyz} \\ \beta_{izx} & \beta_{izy} & \beta_{izz} \end{pmatrix} \begin{pmatrix} E_{loc,x}^\omega \\ E_{loc,y}^\omega \\ E_{loc,z}^\omega \end{pmatrix} \\ &\quad + (\alpha_{ix}^{2\omega} \ \alpha_{iy}^{2\omega} \ \alpha_{iz}^{2\omega}) \begin{pmatrix} E_{loc,x}^{2\omega} \\ E_{loc,y}^{2\omega} \\ E_{loc,z}^{2\omega} \end{pmatrix} \end{aligned} \quad (2)$$

Here α_{ij} is the linear polarizability tensor and β_{ijk} is the second order nonlinear polarizability tensor of the each molecule in the laboratory coordinates $\lambda(x, y, z)$ with the index ijk as either one of the three laboratory Cartesian coordinates. The first term in the Eq.2 is the linear induced dipole, the second term is the induced dipole at the second harmonic frequency (2ω) induced by the field with the fundamental frequency ω through the second harmonic process, and the third term is the induced dipole at 2ω induced by the field with 2ω through a linear process. The field with 2ω in the third term is the result of the second term. The molecular polarizability tensors in the laboratory coordination $\lambda(x, y, z)$ can be projected from the molecular polarizability tensors in the molecular coordination $\lambda'(a, b, c)$.

The above is general for any dielectric medium. In the problem we describe below, only the induced dipoles at the interface with the fundamental and second harmonic frequency are considered. The case for the sum-frequency works similarly following the same approach. For the isotropic molecular monolayer, there are two independent linear optical polarizability tensors in the laboratory coordination $\lambda(x, y, z)$, $\alpha_{xx} = \alpha_{yy}$, and α_{zz} ; and there are three non-vanishing independent β elements, $\beta_{xxz} = \beta_{yyz} = \beta_{zzx} = \beta_{zyz}$, $\beta_{zxx} = \beta_{zyy}$ and β_{zzz} .^{25,53} Now the induce dipole moment of each molecule can be written explicitly as

$$\begin{aligned}
\mu_x^\omega &= \alpha_{xx}^\omega E_{loc,x}^\omega \\
\mu_y^\omega &= \alpha_{yy}^\omega E_{loc,y}^\omega \\
\mu_z^\omega &= \alpha_{zz}^\omega E_{loc,z}^\omega \\
\mu_x^{2\omega} &= \alpha_{xx}^{2\omega} E_{loc,x}^{2\omega} + \beta_{xxz} E_{loc,x}^\omega E_{loc,z}^\omega + \beta_{xzx} E_{loc,z}^\omega E_{loc,x}^\omega \\
\mu_y^{2\omega} &= \alpha_{yy}^{2\omega} E_{loc,y}^{2\omega} + \beta_{yyz} E_{loc,y}^\omega E_{loc,z}^\omega + \beta_{yzy} E_{loc,z}^\omega E_{loc,y}^\omega \\
\mu_z^{2\omega} &= \alpha_{zz}^{2\omega} E_{loc,z}^{2\omega} + \beta_{zxx} E_{loc,x}^\omega E_{loc,x}^\omega + \beta_{zyy} E_{loc,y}^\omega E_{loc,y}^\omega + \beta_{zzz} E_{loc,z}^\omega E_{loc,z}^\omega
\end{aligned} \tag{3}$$

Now, in order to calculate these induced dipoles of the monolayer, the knowledge of the local fields \vec{E}_{loc}^ω and $\vec{E}_{loc}^{2\omega}$ at the interface needs to be described.

When an optical field is incident on a molecular monolayer at the interface between two bulk phases with dielectric constant $\varepsilon_1 = n_1^2$ and $\varepsilon_2 = n_2^2$, the induced dipole in the monolayer and the image induced dipole in the substrate all add to the local field at each individual molecule within the monolayer. Therefore the total local field is different from the applied electric field. Then,^{56,88,89}

$$\vec{E}_{loc}(\vec{r}) = \vec{E}(\vec{r}) + \vec{E}_{dip}(\vec{r}) + \vec{E}_{dip,I}(\vec{r}) \tag{4}$$

Here, let \vec{r} be the position vector within the monolayer from the center of the molecule at the origin position. Then $\vec{E}_{loc}(\vec{r})$ is the local field at \vec{r} , and it is the sum of three contributions. Here $\vec{E}(\vec{r})$ is the applied field, $\vec{E}_{dip}(\vec{r})$ is the field acted at this point from all the induced dipoles except the one at \vec{r} , and $\vec{E}_{dip,I}(\vec{r})$ is the field created by all the image induced dipoles at \vec{r} .

Here we first discuss the first term $\vec{E}(\vec{r})$. In this case, a field of plane wave at frequency ω is incident at an angle of α_i upon the interface from one bulk phase and reflected from the interface. Because the applied field is not with frequency 2ω , one always have $\vec{E}(\vec{r}, 2\omega) = 0$. For $\vec{E}(\vec{r}, \omega)$, because of the existence of the interface, the applied electric field is the superposition of the incident field plus the field reflected from the interface.^{56,88,89} According to the Fresnel formulae,⁸⁴ the total applied field $\vec{E}(\vec{r}, \omega)$ (E_x, E_y, E_z) can be determined from the incident electric field $\vec{E}_0(E_{0,x}, E_{0,y}, E_{0,z}) = E_0 \hat{e}$ as followings:

$$\begin{aligned}
E_x &= (1 - r_p e^{i2k_1 d \cos \Omega_i}) E_{x,0} = \left(1 + \frac{n_1 \cos \Omega_t - n_2 \cos \Omega_i}{n_2 \cos \Omega_i + n_1 \cos \Omega_t} e^{i2k_1 d \cos \Omega_i}\right) E_{x,0} = L'_{xx} E_{x,0} \\
E_y &= (1 + r_s e^{i2k_1 d \cos \Omega_i}) E_{x,0} = \left(1 + \frac{n_1 \cos \Omega_i - n_2 \cos \Omega_t}{n_1 \cos \Omega_i + n_2 \cos \Omega_t} e^{i2k_1 d \cos \Omega_i}\right) E_{y,0} = L'_{yy} E_{y,0} \\
E_z &= (1 + r_p e^{i2k_1 d \cos \Omega_i}) E_{x,0} = \left(1 + \frac{n_2 \cos \Omega_i - n_1 \cos \Omega_t}{n_2 \cos \Omega_i + n_1 \cos \Omega_t} e^{i2k_1 d \cos \Omega_i}\right) E_{z,0} = L'_{zz} E_{z,0}
\end{aligned} \tag{5}$$

This may be simplified as $\vec{E} = [\mathbb{L}' \cdot \hat{e}] E_0$. Here, Ω_i and Ω_t are the incident angle and the refraction angle at the interface. k_1 is the wave vector in first bulk phase, d is the distance of the dipole from the interface. Generally for the monolayer $d \ll \lambda$, $e^{i2k_1 d \cos \Omega_i} \sim 1$. In this case, the expression of the Fresnel factor L'_{ii} is simplified into L_{ii} , which will be expressed in the Section III.

The expression of $\vec{E}(\vec{r})$ in the Eq.5 is independent from the structure of the interfacial monolayer for any interface between two isotropic bulk phases. However, the expressions of the other two terms in the Eq.4 depend on the model of the monolayer structure. In order to evaluate them, here a square lattice model is used to represent the molecular monolayer. Other kinds of lattice models, such as the hexagonal lattice model, can also be employed and they shall generate similar results.^{90,91} Here we only discuss the case using the square lattice model.

Bagchi et al^{88,89} and Ye et al⁵⁶ used the classical discrete square point-dipole model to discuss the linear and nonlinear optical responses of the molecular monolayer, respectively. Such a square lattice model is illustrated in Fig.1. The dipoles at the interface forms a two-dimensional square lattice with a lattice constant a . The two bulk phases occupy the two semi-infinite space of $z \geq 0$ and $z \leq 0$ respectively, and they are characterized by the bulk dielectric constant ϵ_1 and ϵ_2 (the substrate), respectively. The tilt angle of the dipole with the surface normal is θ and its azimuthal orientation is randomly distributed in the plane of the interface. The distance of the point dipole to the lower substrate surface is d . The coordinates of each point dipole is then $\vec{R}_{m,n} = (ma, na, d)$, where m and n are integer indexes along the x and y directions from the origin $O(0, 0, 0)$ in the plane of the monolayer, respectively.

The contribution to the dipolar field $\vec{E}_{dip}(\vec{r})$ at an adsorbed dipole comes from the neighboring induced dipoles within the monolayer.⁸⁹ As in previous treatments,^{56,88,89} the near field approximation of the local field is employed.

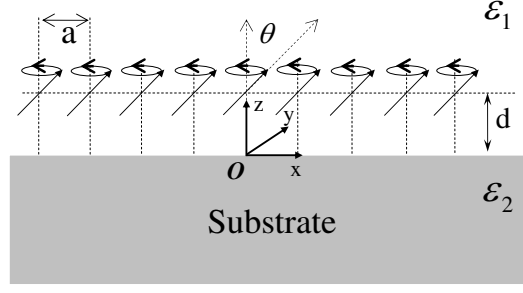


FIG. 1: Illustration of an infinite lattice of point induced dipoles on a substrate interface. a is the distance between the nearest molecules, or the lattice constant; d is the distance from the center of the point-dipole to the surface of the substrate; θ is the tilt angle of the point-dipoles.

In the near field approximation, the magnetic part of the electromagnetic field is ignored, and the retardation effects are discarded.^{77,88,89} This assumption is justified because the wavelength λ of the incident electric field is much larger than the lattice constant a . Following the works by Bagchi, the electric field at the lattice point $R_{00}(0, 0, d)$ which is created by the rest of the induced-dipoles in the lattice plane is^{88,89}

$$\begin{aligned} E_{dip}^{R_{00}} &= \sum_{m,n=-\infty}^{\infty} ', \frac{3 [\vec{\mu} \cdot (\vec{R}_{mn} - \vec{R}_{00})] (\vec{R}_{mn} - \vec{R}_{00}) - \vec{\mu} (\vec{R}_{mn} - \vec{R}_{00})^2}{(\vec{R}_{mn} - \vec{R}_{00})^5} \\ &= \hat{z} \left(\frac{\mu_z}{a^3} \right) \xi_0 - \left[\hat{x} \left(\frac{\mu_x}{a^3} \right) + \hat{y} \left(\frac{\mu_y}{a^3} \right) \right] \frac{\xi_0}{2} \end{aligned} \quad (6)$$

The CGS unit system is used in this paper, as in many textbooks. Here μ_i is the components of the induced dipole $\vec{\mu}$. \hat{x} , \hat{y} , and \hat{z} are the unit vectors in the laboratory coordinates. The symbol prime ' denotes that the summation does not include the point of origin R_{00} . The constant ξ_0 was evaluated by Topping in 1927.⁹¹

$$\xi_0 = - \sum_{m,n=-\infty}^{\infty} ' (m^2 + n^2)^{-\frac{3}{2}} = -9.0336 \quad (7)$$

In the Eq.6, only the induced dipole in the same plane of the interface lattice is considered. To be more rigorous, molecular layers other than the interface lattice plane also need to be considered. These layers may be the molecules or atoms of the two bulk phases, whose polarizabilities differ from those of the dipoles in the interfacial layers. Phenomenologically, let's define a vertical lattice index l and lattice constant d_l , with $l = 0$ for the plane of the monolayer rather than the plane with the origin $O(0, 0, 0)$. Then the total $\vec{E}_{dip}(\vec{r}) = E_{dip}^{R_{00}} + E_{dip}^{R_{00}, l \neq 0}$, with $E_{dip}^{R_{00}, l \neq 0}$ as the induced dipole interaction contribution to the $R_{00}^0 = R_{00}$ origin point from the induced dipoles other than the interface lattice plane.

$$\begin{aligned} E_{dip}^{R_{00}, l \neq 0} &= \sum_{l=-\infty}^{\infty} ', \sum_{m,n=-\infty}^{\infty} \frac{3 [\vec{\mu}^l \cdot (\vec{R}_{mn}^l - \vec{R}_{00}^0)] (\vec{R}_{mn}^l - \vec{R}_{00}^0) - \vec{\mu}^l (\vec{R}_{mn}^0 - \vec{R}_{00}^0)^2}{(\vec{R}_{mn}^l - \vec{R}_{00}^0)^5} \\ &= \sum_{l=-\infty}^{\infty} ', \left(\hat{z} \left(\frac{\mu_z^l}{a_l^3} \right) \xi_0^l - \left[\hat{x} \left(\frac{\mu_x^l}{a_l^3} \right) + \hat{y} \left(\frac{\mu_y^l}{a_l^3} \right) \right] \frac{\xi_0^l}{2} \right) \end{aligned} \quad (8)$$

Here a_l is the lattice constant of the l layer. The expression here is similar to the expressions for the image dipole term by Bagchi and Ye et al.^{56,88,89} Here ξ_0^l can be directly derived from the Eq.6.

$$\xi_0^l = \sum_{m,n=-\infty}^{\infty} \frac{3 (2ld/a_l)^2 - [m^2 + n^2 + (2ld/a_l)^2]}{[m^2 + n^2 + (2ld/a_l)^2]^{5/2}} \quad (9)$$

To evaluate how quickly this summation converges with increase of l , it can be converted into a more rapidly convergent series.^{88,89}

$$\xi_0^l = 16\pi^2 \sum_{m=0}^{\infty} \sum_{n=1}^{\infty} (m^2 + n^2)^{1/2} \exp \left[-4\pi l \left(\frac{d}{a_l} \right) (m^2 + n^2)^{1/2} \right] \quad (10)$$

The Eq.10 indicates that ξ_0^l falls off exponentially as the l increases. Generally, when $d \sim a/2$, even the contribution of the immediate neighboring layer, i.e. $l = \pm 1$ can be neglected. This is the basis for the planewise dipole sum rule in the molecular crystal theory, which shall be discussed in the Section IV.^{73,74,75,76,77,78} The planewise sum rule in the molecular crystal theory concluded that the contribution of the induced dipoles from neighboring layers contribute insignificantly to the local field of the induced dipoles in the layer under consideration, comparing to that from the induced dipoles in the same layer.

The image dipole contribution is just a special case in the Eq.8. Bagchi and Ye *et al.* discussed and evaluated the image dipole contributions previously.^{56,88,89} The image dipoles is located in the substrate at $\vec{R}'_{mn} = (ma, nb, -d)$, i.e. $l = -2$ in the general case above, and the image dipole is defined as^{56,88,89}

$$\begin{aligned}\mu_I(\omega)_x &= \frac{\epsilon_2 - \epsilon_1}{\epsilon_2 + \epsilon_1}(-\mu_x) \\ \mu_I(\omega)_y &= \frac{\epsilon_2 - \epsilon_1}{\epsilon_2 + \epsilon_1}(-\mu_y) \\ \mu_I(\omega)_z &= \frac{\epsilon_2 - \epsilon_1}{\epsilon_2 + \epsilon_1}(\mu_z)\end{aligned}\quad (11)$$

Thus, the image dipole contribution can also be calculated as the same procedure as in the Eq.8.^{56,88,89} Ye and Shen concluded that for the typical case on a metal surface, where $(\epsilon_2 - \epsilon_1)/(\epsilon_2 + \epsilon_1) \sim 1$, when $d \geq 2.5\text{\AA}$ with $a = 5\text{\AA}$, the image induced dipole contribution is negligible.⁵⁶ Therefore, it is generally accepted that for the dielectric substrate, where $(\epsilon_2 - \epsilon_1)/(\epsilon_2 + \epsilon_1) \ll 1$, this image induced dipole term needs not to be considered.^{43,44,45,46,47,48,49,50,51,81} Therefore, we shall neglect the image induced dipole term in the followed treatment.

It has to be noted that both the $\vec{E}_{dip}(\vec{r})$ and the $\vec{E}_{dip,I}(\vec{r})$ terms have the same expressions for the fundamental and second harmonic frequencies.

With all the three terms known from above, put the Eq.4, the Eq.6 the Eq.8 into the Eq.3, one has

$$\begin{aligned}\mu_x^\omega &= \alpha_{xx}^\omega l_{xx}(\omega) E_x \\ \mu_y^\omega &= \alpha_{yy}^\omega l_{yy}(\omega) E_y \\ \mu_z^\omega &= \alpha_{zz}^\omega l_{zz}(\omega) E_z \\ \mu_x^{2\omega} &= l_{xx}(2\omega) \beta_{xxz} l_{xx}(\omega) l_{zz}(\omega) E_x^\omega E_z^\omega + l_{xx}(2\omega) \beta_{xxz} l_{zz}(\omega) l_{xx}(\omega) E_z^\omega E_x^\omega \\ \mu_y^{2\omega} &= l_{yy}(2\omega) \beta_{yyz} l_{yy}(\omega) l_{zz}(\omega) E_y^\omega E_z^\omega + l_{yy}(2\omega) \beta_{yyz} l_{zz}(\omega) l_{yy}(\omega) E_z^\omega E_y^\omega \\ \mu_z^{2\omega} &= l_{zz}(2\omega) \beta_{zzx} l_{xx}(\omega) l_{xx}(\omega) E_x^\omega E_z^\omega + l_{zz}(2\omega) \beta_{zzx} l_{xx}(\omega) l_{zz}(\omega) E_x^\omega E_z^\omega \\ &\quad + l_{zz}(2\omega) \beta_{zzz} l_{zz}(\omega) l_{zz}(\omega) E_z^\omega E_z^\omega\end{aligned}\quad (12)$$

Here the E_i^ω is from the Eq.5, and l_{ii} is the microscopic local field factors for the isotropic monolayer using the discrete induced dipole model. l_{ii} is explicitly derived and is defined as below.⁵⁶

$$\begin{aligned}l_{xx}(\omega_i) &= \left[1 + \frac{\alpha_{xx}^{\omega_i}}{2a^3} \xi_0 + \sum_{l=-\infty}^{\infty} ' \frac{\alpha_{xx}^{l,\omega_i}}{2a_l^3} \xi_0^l \right]^{-1} \\ l_{yy}(\omega_i) &= \left[1 + \frac{\alpha_{yy}^{\omega_i}}{2a^3} \xi_0 + \sum_{l=-\infty}^{\infty} ' \frac{\alpha_{yy}^{l,\omega_i}}{2a_l^3} \xi_0^l \right]^{-1} \\ l_{zz}(\omega_i) &= \left[1 - \frac{\alpha_{zz}^{\omega_i}}{a^3} \xi_0 - \sum_{l=-\infty}^{\infty} ' \frac{\alpha_{zz}^{l,\omega_i}}{a_l^3} \xi_0^l \right]^{-1}\end{aligned}\quad (13)$$

Here $\omega_i = \omega$ or 2ω , and $\alpha_{ii}^{\omega_i}$ is the linear polarizability tensor which can be calculated from the molecular polarizability values in the molecular coordinates frame $\lambda'(a, b, c)$. The summation term in the Eq.13 is the dipole interaction from layers other than the interface layer, which are generally negligible. However, in the Section IV, the form shall be used in the discussion of the segmentation of the chain molecules in the molecular monolayer. The $\xi_0 = -9.0336$ is for the square lattice model as derived by Topping.⁹¹ Since ξ_0 is negative, $l_{xx} = l_{yy}$ is generally larger than unity, while l_{zz} is smaller than unity. However, when a is small, $|\alpha_{xx}^{\omega_i} \xi_0 / 2a^3| > 1$ can happen, this would result in negative $l_{xx} = l_{yy}$ values even under the normal dispersion condition for the bulk material. This is unique for the two-dimensional cases.

The molecular polarizability at the experimental coordinates can be expressed as from the coordinates transition relation: $\alpha_{ij} = \sum_{i',j'=a,b,c} R_{ii'} R_{jj'} \alpha_{i'j'}$, with $R_{\lambda,\lambda'}$ as the element of the rotational transformation matrix from the molecular coordination $\lambda'(a, b, c)$ to the laboratory coordination $\lambda(x, y, z)$.^{21,92} For the ensemble of rotationally isotropic monolayer in the x-y plane, each individual molecule possesses the same homogeneous distribution in the

azimuthal orientation and the twist orientation. Then, one has

$$\begin{aligned}\alpha_{xx} &= \frac{1}{4} \cdot (1 + \cos^2 \theta) \cdot \alpha_{aa} + \frac{1}{4} \cdot (1 + \cos^2 \theta) \cdot \alpha_{bb} + \frac{1}{2} \cdot \sin^2 \theta \cdot \alpha_{cc} \\ \alpha_{yy} &= \frac{1}{4} \cdot (1 + \cos^2 \theta) \cdot \alpha_{aa} + \frac{1}{4} \cdot (1 + \cos^2 \theta) \cdot \alpha_{bb} + \frac{1}{2} \cdot \sin^2 \theta \cdot \alpha_{cc} \\ \alpha_{zz} &= \frac{1}{2} \cdot \sin^2 \theta \cdot \alpha_{aa} + \frac{1}{2} \cdot \sin^2 \theta \cdot \alpha_{bb} + \cos^2 \theta \cdot \alpha_{cc}\end{aligned}\quad (14)$$

Here we did not consider the case when the tilt angle θ is with a distribution. In that case, the Eq.14 need to be put into the form with ensemble average over the distribution of θ . In doing calculations, the polarizability of the molecule or molecular groups can be obtained from many compiled sources,^{93,94,95} or from direct quantum mechanics calculations.

The local field corrected linear and nonlinear polarizabilities in the Eq.12 are the source of the linear or nonlinear radiations from the monolayer at the interface. Their detail expressions will not appear in the next section when we try to calculate the total radiation from the monolayer. The detailed expression in the Eq.12, the Eq.13, and the Eq.14 can be used for direct calculation of the local field factors and the local field corrected polarizabilities in general.

The expression in the Eq.13, can be slightly different if a non-square lattice model is assumed. For other geometries, for example, the hexagonal or equi-triangular geometry, the calculation of different geometries can be put forward according to Topping's treatment.⁹¹

The Eq.13 clearly indicates that when the distance a between the neighboring molecules in the monolayer becomes large, i.e. the submonolayer case, the l_{ii} value is approaching unity very quickly. This actually defines the meaning of the word 'local', by considering how rapid the value ξ_0 is converged when doing summation of the dipoles in the lattice plane over m and n . According to Topping and Philpott's calculations, the convergence is generally reached in the 4th digit before $m, n < 10$.^{77,91} For a lattice constant of $a = 5\text{\AA}$, this means the local field calculation converges within 5nm. Since when a become large, the local field factors in the Eq.13 decays to unity rapidly, therefore, the local field can be viewed as localized interactions with few nanometers. The planewise sum rule also restricts the local field effect within only a few Angstroms from the dipole under consideration. These facts provide definition of the actual range of the local field effects.

By introducing the microscopic local field factors, the calculation of the response from an ensemble of induced dipoles to an electromagnetic field is reduced to a calculation of the response of the isolated molecule interacting with the local field.

III. SECOND HARMONIC RADIATION FROM THE DISCRETE INTERFACE INDUCED DIPOLES IN THE FAR FIELD

Here we present the calculate of the linear and second harmonic radiation in the far field according to the two-dimensional lattice of the local field corrected induced dipoles at an interface between the two isotropic bulk phases. The calculation using the square lattice model can also be performed with hexagonal or other lattice models. We shall see that since the radiation in the far field is additive for the radiating dipoles, ensemble average treatment of the radiating dipole can be straightforwardly implemented. The following derivation uses the CGS convention, unless specified otherwise.

In this problem, the radiation from the point induced dipole $\vec{\mu}$ at the linear and second harmonic frequencies is in the upper phase (ε_1) in Fig.1. Here the point of origin $O(0,0,0)$ is at the center of the dipole, different from the definition in the previous section. This is for the convenience of calculation in this section. Now, the general field radiated from an electric dipole μ along the z direction, i.e. $\mu\hat{z}$, in the ε_1 phase is⁸⁴

$$\begin{aligned}E_r &= \frac{2\mu k_1^3}{\varepsilon_1} \left\{ \frac{1}{(k_1 r)^3} - \frac{i}{(k_1 r)^2} \right\} \cos \theta e^{i(\vec{k}_1 \cdot \vec{r} - \omega t)} \\ E_\theta &= \frac{\mu k_1^3}{\varepsilon_1} \left\{ \frac{1}{(k_1 r)^3} - \frac{i}{(k_1 r)^2} - \frac{1}{(k_1 r)} \right\} \sin \theta e^{i(\vec{k}_1 \cdot \vec{r} - \omega t)} \\ E_\varphi &= 0\end{aligned}\quad (15)$$

Here μ is the modulus of the induced-dipole, k_1 is the wave vector in phase 1, r is the distance from the point of the dipole to the point of detection at $M(r, \theta, \varphi)$ with θ as the tilt angle and φ as the azimuthal angle in the polar coordinates. If we only consider the far field, which is generally in the experimental measurements except for the near field studies, all the high order $1/r$ terms can be neglected. Therefore, only the $1/r$ term of the E_θ in the Eq.15 need to be considered.

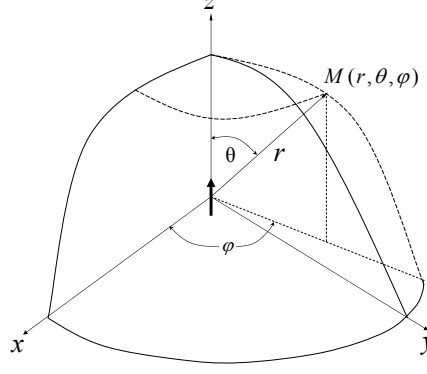


FIG. 2: Polar coordinates with an electric dipole with moment vector along the z-axis. μ is the modulus of the induced-dipole, r is the distance from the point of the dipole to the point of detection, θ is the tilt angle in the polar coordinates, φ is the azimuthal angle.

In the following, the total macroscopic radiation field at a space point $R(0, 0, R_0)$ in the reflection direction can be calculated from the summation of the field of the radiation directly from the individual induced dipole at the interface and the radiated field reflected from the interface. In doing so, the amplitude and phase of the radiated field at $R(0, 0, R_0)$ need to be expressed into the function of the components of individual induced dipole at the interface, before the summation can be carried out over them.

The connection between the induced-dipole components μ_x , μ_y and μ_z and their radiation field components E_x , E_y and E_z at $R(0, 0, R_0)$ is illustrated in Figure 3. The total phase at $R(0, 0, R_0)$ can be calculated by choosing the point of origin $O(0, 0, 0)$ as the reference point. Therefore the phase difference of the radiation field at $R(0, 0, R_0)$ between the dipole at the point $r(ma, na, 0)$ and the fixed point of origin $O(0, 0, 0)$ can be calculated from the difference of the two distances RO and Rr , i.e., $r(m, n) - R_0$, with

$$r(m, n) = \sqrt{(ma)^2 + (na)^2 + (R_0)^2}. \quad (16)$$

Now, the phase difference of the incident field at O and r on the dipole plane also need to be calculated. When a plane wave is incident on the monolayer at the incident angle Ω_i , remembering that the incident plane is xz , and m is along the x direction, this phase difference is $k_1^{in}(ma \sin \Omega_i)$. For the case of second harmonic generation, this phase difference involves two incoming waves, therefore the total phase difference is $2k_1^{in}(ma \sin \Omega_i)$.

Therefore, the total phase at the space point $R(0, 0, R_0)$ is the sum of all these phase differences. If we define this total phase of the radiation from the induced dipole at $r(ma, na, 0)$ at $R(0, 0, R_0)$, as $k_1 f(m, n)$, one has

$$f(m, n) = \sqrt{(ma)^2 + (na)^2 + (R_0)^2} + \frac{\eta k_1^{in}}{k_1} (ma \sin \Omega_i). \quad (17)$$

Here when the radiation frequency is the same as the incoming frequency ω , then $\eta = 1$, and $k_1^{in} = k_1$; while when the radiation frequency is 2ω , then $\eta = 2$, and $k_1^{in} \neq k_1$. More generally, for the case of the sum frequency generation ($\omega_3 = \omega_1 + \omega_2$), the expression of the second term in $f(m, n)$ becomes

$$\frac{ma}{k_1(\omega_3)} [k_1^{in}(\omega_1) \sin \Omega_i^{\omega_1} + k_1^{in}(\omega_2) \sin \Omega_i^{\omega_2}] \quad (18)$$

With the phase known, the radiation field at $R(0, 0, R_0)$ generated from the dipole $\vec{\mu}(\mu_x, \mu_y, \mu_z)$ at $r(ma, na, 0)$ can be calculated separately for each μ_i according to the Eq.15 with proper projection.

Then the field components E_x , E_y , E_z at $R(0, 0, R_0)$ generated by μ_x at $r(ma, na, 0)$ are

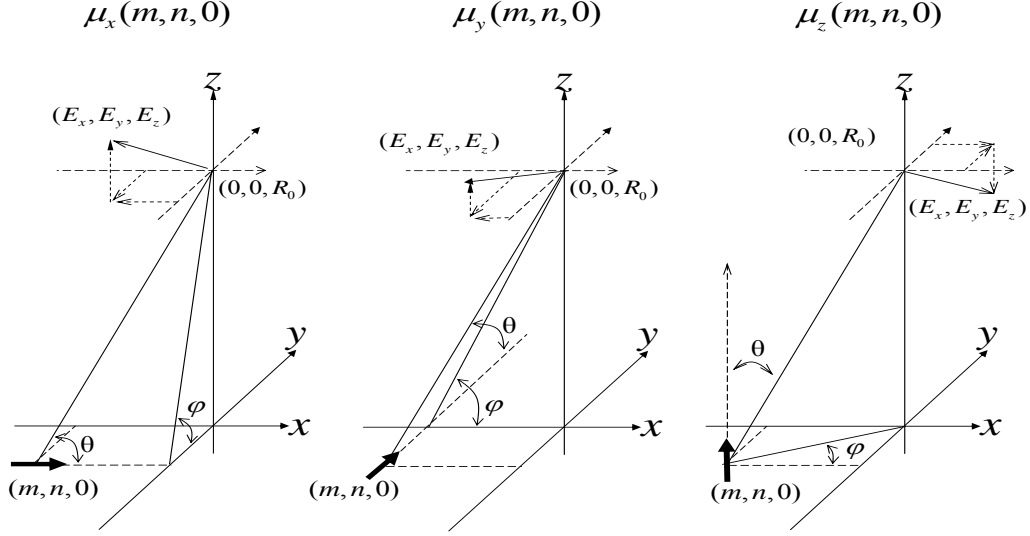


FIG. 3: Calculation of the field vector (E_x, E_y, E_z) , which is created by $\mu_x(m, n, 0)$, $\mu_y(m, n, 0)$, $\mu_z(m, n, 0)$ respectively. θ being the tilt angle of the dipole moment vector, φ being the azimuthal angle of r which is the vector from the point of $(m, n, 0)$ to the point $(0, 0, R_0)$, as illustrated in Fig.2.

$$\begin{aligned}
 E_{\mu_x, x} &= -E_{\mu_x, \theta} \sin \theta = \frac{k_1^2 \sin^2 \theta}{\varepsilon_1 r(m, n)} \mu_x e^{i(k_1 f(m, n) - \omega t)} \\
 E_{\mu_x, y} &= E_{\mu_x, \theta} \cos \theta \cos \varphi = -\frac{k_1^2 \sin \theta \cos \theta \cos \varphi}{\varepsilon_1 r(m, n)} \mu_x e^{i(k_1 f(m, n) - \omega t)} \\
 E_{\mu_x, z} &= E_{\mu_x, \theta} \cos \theta \sin \varphi = -\frac{k_1^2 \sin \theta \cos \theta \sin \varphi}{\varepsilon_1 r(m, n)} \mu_x e^{i(k_1 f(m, n) - \omega t)}
 \end{aligned} \tag{19}$$

with

$$\begin{aligned}
 \sin \theta &= \frac{\sqrt{(na)^2 + R_0^2}}{\sqrt{(ma)^2 + (na)^2 + R_0^2}}, \quad \cos \theta = \frac{-ma}{\sqrt{(ma)^2 + (na)^2 + R_0^2}} \\
 \sin \varphi &= \frac{R_0}{\sqrt{(na)^2 + R_0^2}}, \quad \cos \varphi = \frac{-na}{\sqrt{(na)^2 + R_0^2}}
 \end{aligned} \tag{20}$$

Similarly the field components E_x, E_y, E_z at $R(0, 0, R_0)$ generated by μ_y at $r(ma, na, 0)$ are

$$\begin{aligned}
 E_{\mu_y, x} &= E_{\mu_y, \theta} \cos \theta \cos \varphi = -\frac{k_1^2 \sin \theta \cos \theta \cos \varphi}{\varepsilon_1 r(m, n)} \mu_y e^{i(k_1 f(m, n) - \omega t)} \\
 E_{\mu_y, y} &= -E_{\mu_y, \theta} \sin \theta = \frac{k_1^2 \sin^2 \theta}{\varepsilon_1 r(m, n)} \mu_y e^{i(k_1 f(m, n) - \omega t)} \\
 E_{\mu_y, z} &= E_{\mu_y, \theta} \cos \theta \sin \varphi = -\frac{k_1^2 \sin \theta \cos \theta \sin \varphi}{\varepsilon_1 r(m, n)} \mu_y e^{i(k_1 f(m, n) - \omega t)}
 \end{aligned} \tag{21}$$

with

$$\begin{aligned}
 \sin \theta &= \frac{\sqrt{(ma)^2 + R_0^2}}{\sqrt{(ma)^2 + (na)^2 + R_0^2}}, \quad \cos \theta = \frac{-na}{\sqrt{(ma)^2 + (na)^2 + R_0^2}} \\
 \sin \varphi &= \frac{R_0}{\sqrt{(ma)^2 + R_0^2}}, \quad \cos \varphi = \frac{-ma}{\sqrt{(ma)^2 + R_0^2}}
 \end{aligned} \tag{22}$$

Then the field components E_x, E_y, E_z at $R(0, 0, R_0)$ generated by μ_z at $r(ma, na, 0)$ are

$$\begin{aligned}
E_{\mu_z, x} &= E_{\mu_z, \theta} \cos \theta \cos \varphi = -\frac{k_1^2 \sin \theta \cos \theta \cos \varphi}{\varepsilon_1 r(m, n)} \mu_z e^{i(k_1 f(m, n) - \omega t)} \\
E_{\mu_z, y} &= E_{\mu_z, \theta} \cos \theta \sin \varphi = -\frac{k_1^2 \sin \theta \cos \theta \sin \varphi}{\varepsilon_1 r(m, n)} \mu_z e^{i(k_1 f(m, n) - \omega t)} \\
E_{\mu_z, z} &= -E_{\mu_z, \theta} \sin \theta = \frac{k_1^2 \sin^2 \theta}{\varepsilon_1 r(m, n)} \mu_z e^{i(k_1 f(m, n) - \omega t)}
\end{aligned} \tag{23}$$

with

$$\begin{aligned}
\sin \theta &= \frac{\sqrt{(ma)^2 + (na)^2}}{\sqrt{(ma)^2 + (na)^2 + R_0^2}}, \quad \cos \theta = \frac{R_0}{\sqrt{(ma)^2 + (na)^2 + R_0^2}} \\
\sin \varphi &= \frac{-na}{\sqrt{(ma)^2 + (na)^2}}, \quad \cos \varphi = \frac{-ma}{\sqrt{(ma)^2 + (na)^2}}
\end{aligned} \tag{24}$$

Now the total radiation field at $R(0, 0, R_0)$ generated by the whole monolayer at the interface is the summation over the whole lattice plane $m(-\infty, +\infty)$ and $n(-\infty, +\infty)$.

$$\begin{aligned}
E_x &= \sum_{m=-\infty}^{\infty} \sum_{n=-\infty}^{\infty} (E_{\mu_x, x} + E_{\mu_y, x} + E_{\mu_z, x}) \\
E_y &= \sum_{m=-\infty}^{\infty} \sum_{n=-\infty}^{\infty} (E_{\mu_x, y} + E_{\mu_y, y} + E_{\mu_z, y}) \\
E_z &= \sum_{m=-\infty}^{\infty} \sum_{n=-\infty}^{\infty} (E_{\mu_x, z} + E_{\mu_y, z} + E_{\mu_z, z})
\end{aligned} \tag{25}$$

The summation in the Eq.25 for the total radiation field is in principle the discrete form of the integro-differential equation in the molecular optics.^{83,84} The asymptotic result of this summation can be evaluated by employing the condition of the far field. Because R_0 is very large as compared with the lattice constant a and the wavelength λ , the discrete summations in the Eq.25 is asymptotic to a continuous integration over the variable set $(x, y) = (ma, na)$. In addition, because R_0 is large and so the phase factor $k_1 f(m, n)$ is large, the exponential factors in the Eq.19, 21 and 23 oscillate very rapidly and change their signs many times as the point $r(ma, na, 0)$ explores the domain of integration.⁸⁴ Under these conditions, an asymptotic value of the total electric field (E_x, E_y, E_z) at point $R(0, 0, R_0)$ can be obtained with the application of the following formula, which are derived from the principle of stationary phase. The detail of the stationary phase method can be found in classic textbook by Born and Wolf.⁸⁴

Here by defining the variables $x = ma$ and $y = na$ with the lattice constant a as a very small quantity compared to the infinity size of the lattice plane, each term in the summation as shown in the Eq.25 becomes the following integral and this integral is then asymptotic to the summation of the stationary phase terms as below.

$$\frac{1}{a^2} \int_{-\infty}^{\infty} \int_{-\infty}^{\infty} g(x, y) e^{ik_1 f(x, y)} dx dy = \frac{2\pi i}{k_1 a^2} \sum_j \frac{\sigma_j}{\sqrt{|\alpha_j \beta_j - \gamma_j^2|}} g(x_j, y_j) e^{ik_1 f(x_j, y_j)} \tag{26}$$

Here $g(x, y)$ is the pre-exponential factors in the Eq.19, 21 and 23. (x_j, y_j) is the points in the whole integration domain at which f is stationary, i.e.

$$\frac{\partial f}{\partial x} = \frac{\partial f}{\partial y} = 0 \tag{27}$$

The definition of the other terms are the followings.

$$\alpha_j = \left(\frac{\partial^2 f}{\partial x^2} \right)_{x_j, y_j}, \quad \beta_j = \left(\frac{\partial^2 f}{\partial y^2} \right)_{x_j, y_j}, \quad \gamma_j = \left(\frac{\partial^2 f}{\partial x \partial y} \right)_{x_j, y_j} \tag{28}$$

and

$$\sigma_j = \begin{cases} +1 & \text{if } \alpha_j \beta_j > \gamma_j^2, \quad \alpha_j > 0, \\ -1 & \text{if } \alpha_j \beta_j > \gamma_j^2, \quad \alpha_j < 0, \\ -i & \text{if } \alpha_j \beta_j < \gamma_j^2. \end{cases} \tag{29}$$

Using the stationary phase condition in the Eq.27 and the expression of f in the Eq.17, a single stationary point (x_1, y_1) is obtained, and

$$x_1 = -R_0 \tan \Omega \quad , \quad y_1 = 0 \quad . \quad (30)$$

Here $\Omega = \Omega_i$ is the direct results of the stationary phase condition for the linear radiation, and for the second harmonic radiation Ω has to satisfy the relationship $k_1(2\omega) \sin \Omega = 2k_1^{in}(\omega) \sin \Omega_i$. Similarly, one can also show explicitly that for the sum frequency radiation, Ω has to satisfy the relationship $k_1(\omega_3) \sin \Omega = k_1^{in}(\omega_1) \sin \Omega_i^{\omega_1} + k_1^{in}(\omega_2) \sin \Omega_i^{\omega_2}$. These are just the condition for the general law of reflection in linear and nonlinear optics, as given by Bloembergen and Pershan, as derived from the Maxwell boundary conditions.³⁵ From these results we shall show later that at the far field space point $R(0, 0, R_0)$, the radiation field is in the direction of Ω , which satisfies the general law of reflection in linear and nonlinear optics. It is interesting that these conditions came incidentally as a solution from the molecular optics treatment. This fact further illustrates the general equivalency of the macroscopic Maxwell equations with boundary conditions and the molecular optics treatment.^{83,84}

Now with the stationary phase point value, we have

$$\begin{aligned} f(x_1, y_1) &= R_0 \cos \Omega \\ \frac{\sigma_1}{\sqrt{|\alpha_1 \beta_1 - \gamma_1^2|}} &= \frac{R_0}{\cos^2 \Omega} \quad . \end{aligned} \quad (31)$$

Here $\sigma_1 = 1$ because $\alpha_1 > 0$ and $\alpha_1 \beta_1 - \gamma_1^2 > 0$. Now put all these values into the expressions in the Eq.25, we have the radiation field components at the space point $R(0, 0, R_0)$ that are directly radiated from the whole induced dipole lattice as the followings.

$$\begin{aligned} E_x^{R_1} &= \frac{2\pi}{a^2 \varepsilon_1} i k_1 (\mu_x \cos \Omega - \mu_z \sin \Omega) e^{i(k_1 R_0 \cos \Omega - \omega t)} \\ E_y^{R_1} &= \frac{2\pi}{a^2 \varepsilon_1} i k_1 \frac{\mu_y}{\cos \Omega} e^{i(k_1 R_0 \cos \Omega - \omega t)} \\ E_z^{R_1} &= \frac{2\pi}{a^2 \varepsilon_1} i k_1 \left(-\mu_x \sin \Omega + \mu_z \frac{\sin^2 \Omega}{\cos \Omega} \right) e^{i(k_1 R_0 \cos \Omega - \omega t)} \end{aligned} \quad (32)$$

In order to calculate the total radiated field at $R(0, 0, R_0)$, besides the direct radiation from the induced dipoles at the interface, the radiation in the forward direction which is reflected from the interface also need to be evaluated. The above procedures can be repeated to calculate the radiated field at the image point $R_i(0, 0, -R_0)$ in the isotropic phase ε_1 from the whole induced dipole lattice. We have

$$\begin{aligned} E_x^{T_1} &= \frac{2\pi}{a^2 \varepsilon_1} i k_1 (\mu_x \cos \Omega + \mu_z \sin \Omega) e^{i(k_1 R_0 \cos \Omega - \omega t)} \\ E_y^{T_1} &= \frac{2\pi}{a^2 \varepsilon_1} i k_1 \frac{\mu_y}{\cos \Omega} e^{i(k_1 R_0 \cos \Omega - \omega t)} \\ E_z^{T_1} &= \frac{2\pi}{a^2 \varepsilon_1} i k_1 \left(\mu_x \sin \Omega + \mu_z \frac{\sin^2 \Omega}{\cos \Omega} \right) e^{i(k_1 R_0 \cos \Omega - \omega t)} \end{aligned} \quad (33)$$

Because the choice of the space point $R(0, 0, R_0)$ and $R_i(0, 0, -R_0)$ is rather arbitrary, and the radiation field components in the Eq.32 and the Eq.33 are both directional and the amplitudes of both plane waves are independent from the value of R_0 , the coherence of the radiation from the induced dipole lattice is conserved at the far field.

According to the Fresnel formulae,⁸⁴ the amplitudes of the reflected electric field components are

$$\begin{aligned} E_x^{R_2} &= -r_p E_x^{T_1} = \frac{n_1 \cos \Omega_t - n_2 \cos \Omega_i}{n_2 \cos \Omega_i + n_1 \cos \Omega_t} E_x^{T_1} \\ E_y^{R_2} &= r_s E_y^{T_1} = \frac{n_1 \cos \Omega_i - n_2 \cos \Omega_t}{n_1 \cos \Omega_i + n_2 \cos \Omega_t} E_y^{T_1} \\ E_z^{R_2} &= r_p E_z^{T_1} = \frac{n_2 \cos \Omega_i - n_1 \cos \Omega_t}{n_2 \cos \Omega_i + n_1 \cos \Omega_t} E_z^{T_1} \end{aligned} \quad (34)$$

The phase difference between the direct radiation field and the reflected field is determined by the distance between the dipole layer and the interface d and the radiation angle Ω as $2k_1 d \cos \Omega$. Therefore the total radiation field at $R(0, 0, R_0)$ is the phase shifted sum of the E^{R_1} and E^{R_2} fields in the Eq.32 and the Eq.34. We have

$$\begin{aligned}
E_{x, total} &= \frac{2\pi}{a^2 \varepsilon_1} i k_1 (\mu_x \cos \Omega - \mu_z \sin \Omega - r_{2p} (\mu_x \cos \Omega + \mu_z \sin \Omega) e^{i 2 k_1 d \cos \Omega}) e^{i (k_1 R_0 \cos \Omega - \omega t)} \\
&= \frac{2\pi}{a^2 \varepsilon_1} i k_1 (\cos \Omega L'_{xx} \mu_x - \sin \Omega L'_{zz} \mu_z) e^{i (k_1 R_0 \cos \Omega - \omega t)} \\
E_{y, total} &= \frac{2\pi}{a^2 \varepsilon_1} i k_1 \left(\frac{\mu_y}{\cos \Omega} + r_{2s} \frac{\mu_y}{\cos \Omega} e^{i 2 k_1 d \cos \Omega} \right) e^{i (k_1 R_0 \cos \Omega - \omega t)} \\
&= \frac{2\pi}{a^2 \varepsilon_1} i k_1 \left(\frac{1}{\cos \Omega} L'_{zz} \mu_y \right) e^{i (k_1 R_0 \cos \Omega - \omega t)} \\
E_{z, total} &= \frac{2\pi}{a^2 \varepsilon_1} i k_1 \left(-\mu_x \sin \Omega + \mu_z \frac{\sin^2 \Omega}{\cos \Omega} + r_{2s} (\mu_x \sin \Omega + \mu_z \frac{\sin^2 \Omega}{\cos \Omega}) e^{i 2 k_1 d \cos \Omega} \right) e^{i (k_1 R_0 \cos \Omega - \omega t)} \\
&= \frac{2\pi}{a^2 \varepsilon_1} i k_1 \left(-\sin \Omega L'_{xx} \mu_x + \frac{\sin^2 \Omega}{\cos \Omega} L'_{zz} \mu_z \right) e^{i (k_1 R_0 \cos \Omega - \omega t)} \tag{35}
\end{aligned}$$

Here the induced dipole components μ_x, μ_y , and μ_z are as defined in the Eq.12, and the L'_{ii} are as defined in the Eq.5. Considering the fact that the thickness of the monolayer is generally much smaller than the magnitude of the optical wavelength, i.e. $d \ll \lambda$, the phase factor $e^{i 2 k_1 d \cos \Omega} \rightarrow 1$. Therefore, L'_{ii} becomes

$$\begin{aligned}
L_{xx} &= \frac{2n_1 \cos \Omega_t}{n_2 \cos \Omega_i + n_1 \cos \Omega_t} = \frac{2\varepsilon_1 k_{2z}}{\varepsilon_2 k_{1z} + \varepsilon_1 k_{2z}} \\
L_{yy} &= \frac{2n_1 \cos \Omega_i}{n_1 \cos \Omega_i + n_2 \cos \Omega_t} = \frac{2k_{1z}}{k_{1z} + k_{2z}} \\
L_{zz} &= \frac{2n_2 \cos \Omega_i}{n_2 \cos \Omega_i + n_1 \cos \Omega_t} = \frac{2\varepsilon_2 k_{1z}}{\varepsilon_2 k_{1z} + \varepsilon_1 k_{2z}} \tag{36}
\end{aligned}$$

These L_{ii} values are clearly the results for the two phase model. This indicates explicitly that when dealing with the macroscopic electric field at the interface, the existence of the interfacial molecular monolayer has minimum influence on the macroscopic field. Therefore, the problem of the linear macroscopic dielectric constant for the interface layer is not a issue in this treatment. This shall be discussed in detail in the Section IV.A.

Now the radiation field components in the second harmonic frequency are

$$\begin{aligned}
E_x^{2\omega} &= \frac{2\pi}{a^2 \varepsilon_1 (2\omega)} i k_1^{2\omega} (\cos \Omega_{2\omega} L_{xx}^{2\omega} \mu_x^{2\omega} - \sin \Omega_{2\omega} L_{zz}^{2\omega} \mu_z^{2\omega}) e^{i (k_1^{2\omega} R_0 \cos \Omega_{2\omega} - 2\omega t)} \\
E_y^{2\omega} &= \frac{2\pi}{a^2 \varepsilon_1 (2\omega)} i k_1^{2\omega} \left(\frac{1}{\cos \Omega_{2\omega}} L_{zz}^{2\omega} \mu_y^{2\omega} \right) e^{i (k_1^{2\omega} R_0 \cos \Omega_{2\omega} - 2\omega t)} \\
E_z^{2\omega} &= \frac{2\pi}{a^2 \varepsilon_1 (2\omega)} i k_1^{2\omega} \left(-\sin \Omega_{2\omega} L_{xx}^{2\omega} \mu_x^{2\omega} + \frac{\sin^2 \Omega_{2\omega}}{\cos \Omega_{2\omega}} L_{zz}^{2\omega} \mu_z^{2\omega} \right) e^{i (k_1^{2\omega} R_0 \cos \Omega_{2\omega} - 2\omega t)} \tag{37}
\end{aligned}$$

Here $k_1^{2\omega} = 2\omega \sqrt{\varepsilon_1(2\omega)}/c$, where c is the velocity of light in vacuum. Now with the second harmonic field components determined, the intensity of the SH field can be directly calculated by the magnitude of the time averaged Poynting vector as defined below.⁹⁶

$$I(\omega) = \frac{c}{2\pi} \sqrt{\varepsilon_1(\omega)} |E_i(\omega)|^2 \tag{38}$$

Then put the expressions in the Eq.37 and the Eq.12 into the Eq.38, and after taking care of the proper projection coefficients of the fundamental and second harmonic electric fields, we have

$$I(2\omega) = \frac{32\pi^3 \omega^2 \sec^2 \Omega_{2\omega}}{c^3 [\varepsilon_1(2\omega)]^{1/2} \varepsilon_1(\omega)} |\chi_{eff}(2\omega)|^2 I^2(\omega) \tag{39}$$

$$\chi_{eff} = [\mathbb{L}(2\omega) \cdot \hat{e}(2\omega)] \cdot \chi(2\omega) : [\mathbb{L}(\omega) \cdot \hat{e}(\omega)] [\mathbb{L}(\omega) \cdot \hat{e}(\omega)] \tag{40}$$

Here $I(\omega)$ is the intensity of the incident laser beam as defined in the Eq.38, and $\Omega_{2\omega}$ is outgoing angle of the second harmonic radiation from the surface normal. $\varepsilon_1(\omega)$ and $\varepsilon_1(2\omega)$ are the bulk dielectric constants of the upper bulk phase at the frequency ω and 2ω , respectively. $\hat{e}(2\omega)$ and $\hat{e}(\omega)$ are the unit vectors of the electric field at 2ω and ω , respectively. $\mathbb{L}(2\omega)$ and $\mathbb{L}(\omega)$ are the tensorial Fresnel factors for 2ω and ω , respectively, as defined as in

the Eq.36. The scalar property $\chi_{eff}(2\omega)$ is the effective macroscopic second-order susceptibility of the interface. The $\chi(2\omega)$ represents the area-averaged macroscopic second harmonic susceptibility tensors defined as $\chi_{ijk}(2\omega) = l_{ii}(2\omega)l_{jj}(\omega)l_{kk}(\omega)\beta_{ijk}/a^2 = N_s l_{ii}(2\omega)l_{jj}(\omega)l_{kk}(\omega)\langle\beta_{i'j'k'}\rangle$, with a as the lattice constant, N_s as the surface number density, and $\langle \rangle$ represents ensemble average over different orientational distributions.

The expressions in the Eq.37 and the Eq.39 are exactly the same as those in the previous treatment by Heinz and Shen.^{4,34,53,54,55} This indicates that the treatment with the square point-dipole lattice model together with a molecular optics approach is at least phenomenologically correct. It also further validates the treatment in the original literatures.

It can be shown accordingly that for the SFG from the interface, one has

$$I(\omega_{SF}) = \frac{8\pi^3\omega^2 \sec^2 \Omega_{SF}}{c^3[\epsilon_1(\omega_{SF})\epsilon_1(\omega_1)\epsilon_1(\omega_2)]^{1/2}} |\chi_{eff}(\omega_{SF})|^2 I(\omega_1)I(\omega_2) \quad (41)$$

$$\chi_{eff} = [\mathbb{L}(\omega_{SF}) \cdot \hat{e}(\omega_{SF})] \cdot \chi(\omega_{SF}) : [\mathbb{L}(\omega_1) \cdot \hat{e}(\omega_1)][\mathbb{L}(\omega_2) \cdot \hat{e}(\omega_2)] \quad (42)$$

Now, the following general issues need to be discussed.

a. Even though the expressions in the Eq.37 and the Eq.39 were obtained through the square induced dipole lattice model, using other type of plane lattice model gives the same asymptomatic expressions at the far field, except that the area-averaged macroscopic second harmonic susceptibility tensors take slightly different expressions. Certainly, the near field results have to be different for different lattice models, because generally no analytical asymptomatic results can be reached for the near field case. In other words, the molecular optics approach described here can be used to treat the near field cases, this is an clear advantage of the molecular optics approach.

b. Here the area-averaged macroscopic second harmonic susceptibility tensors $\chi_{ijk}(2\omega)$ and the factor $1/a^2$ in the Eq.37 needs to be discussed. a^2 is the average area per induced dipole in the lattice plane under the square induced-dipole lattice model. It comes into the expression naturally because of the summation, or integration, over the whole lattice plane. Therefore, μ_i/a^2 is the area averaged induced dipole, and $\chi_{ijk}(2\omega)$ is the area-averaged macroscopic second harmonic susceptibility tensors. In the previous treatments on second harmonic generation,^{4,54} an infinitesimally thin polarization sheet layer was used, and the polarization for this interface layer was defined in the form of $P(2\omega) = \chi(2\omega)\delta(z) : E(\omega)E(\omega)$, or sometimes $P(2\omega) = \chi(2\omega) : E(\omega)E(\omega)$.^{4,26,54,97} In this way, it is a little confusing when one try to make the dimension analysis of the formulae when trying to apply the interface polarization term into the Maxwell equations. However, in this molecular optics treatment, there is no ambiguity involved, and the $\chi(2\omega)$ tensor has to have the dimension of an area-averaged second order nonlinear polarizability.

c. The ensemble average of the $\chi_{ijk}(2\omega)$ tensors. In calculation of the summation and its asymptomatic results in the far field, the actual size of the lattice constant a can be treated arbitrarily as long as the lattice constant a is microscopic. Because the additive nature of the summation in the Eq.25, it is easy to show that even though the surface is not a square lattice for each individual dipole, one can always divide the surface layer into the square lattice with microscopic unit cells each containing a group of individual neighboring induced dipoles. Therefore, this approach actually allows making ensemble average with each unit cell. It even allow the unit cell to contain several layers of molecules close to the interface region. This further allows the inclusion of the contributions of the quadrupolar and the interfacial discontinuity terms into the effective unit induced dipole cells at the interface region.^{4,26,31,35,97,98} Of course, each of these different treatments has to be involved with different microscopic description and symmetry analysis of the area-averaged effective microscopic polarizability tensor terms χ_{ijk} of the unit cell as defined.

With above issues cleared, now we may say that the Eq.37 and the Eq.39 are general for the second harmonic generation from the whole interface region, with the possibility to make microscopic treatment or calculation with different microscopic models of the interface region. Similar treatment can be performed for the sum frequency generation process from the interface. Its detail is not discussed here.

In the SHG, most of the time a rotationally isotropic molecular interface is studied. If we let α_{in} be the polarization angle of the incident electric field, let γ_{out} be the polarization angle of the second harmonic electric field, $\chi_{eff,\alpha_{in}-\gamma_{out}}$ be the corresponding effective macroscopic nonlinear susceptibility. Then the $\chi_{eff,\alpha_{in}-\gamma_{out}}$ can be expressed into the linear combinations of the three independently measurable terms with the following polarization combinations: $s_{in}-p_{out}$, $45^\circ_{in}-s_{out}$, $p_{in}-p_{out}$, with s as the polarization perpendicular to the incident plane, and p as the polarization in the incident plane. Let Ω_ω and $\Omega_{2\omega}$ be the incoming and outgoing angles, respectively, one has²⁵

$$\chi_{eff,\alpha_{in}-\gamma_{out}} = \chi_{eff,45^\circ-s} \sin \gamma \sin 2\alpha + \chi_{eff,s-p} \cos \gamma \sin^2 \alpha + \chi_{eff,p-p} \cos \gamma \cos^2 \alpha \quad (43)$$

$$\begin{aligned} \chi_{eff,s-p} &= L_{zz}(2\omega)L_{yy}(\omega)L_{yy}(\omega) \sin \Omega_{2\omega} \chi_{zyy} \\ \chi_{eff,45^\circ-s} &= L_{yy}(2\omega)L_{zz}(\omega)L_{yy}(\omega) \sin \Omega_\omega \chi_{yzy} \\ \chi_{eff,p-p} &= -2L_{xx}(2\omega)L_{zz}(\omega)L_{xx}(\omega) \cos \Omega_{2\omega} \sin \Omega_\omega \cos \Omega_\omega \chi_{xzx} \\ &\quad + L_{zz}(2\omega)L_{xx}(\omega)L_{xx}(\omega) \sin \Omega_{2\omega} \cos^2 \Omega_\omega \chi_{zxx} \\ &\quad + L_{zz}(2\omega)L_{zz}(\omega)L_{zz}(\omega) \sin \Omega_{2\omega} \sin^2 \Omega_\omega \chi_{zzz} \end{aligned} \quad (44)$$

Details of the quantitative experimental measurement and interpretation of the interface SHG, as well as the SFG-vibrational spectroscopy, of molecular interfaces with these formulations can be found in the recent literatures.^{21,25}

IV. DISCUSSION

Two of the central issues with general interests in the quantitative interpretation of the SHG and SFG-VS data are whether the molecular monolayer has a linear macroscopic dielectric constant and how the microscopic local field effects is evaluated. Actually previous researchers already provided most of the answers as reviewed in the introduction section above. Because the SHG and the SFG-VS have been proven as the sensitive probes for interfaces with the submonolayer coverage,^{2,4,8,10} the treatment based on the more realistic discrete induced dipole lattice model is developed in this work. Based on the microscopic treatment of the SHG and SFG-VS from the molecular interface, these issues are to be discussed.

A. The linear macroscopic dielectric constant of the molecular monolayer or submonolayer

The concern of the linear macroscopic dielectric constant of the interface is from the beginning of the development of SHG and SFG-VS as the quantitative surface spectroscopic probes.²⁶ Here we quote the following sentences from the Chapter ‘Surface Nonlinear Optics’ in Shen’s classical textbook:²⁶

‘In the usual simplified approach, the surface microscopic layer is assumed to have a characterized thickness with optical constants different from the bulk. Because of the linear transmission and reflection of the light at the boundary surface usually are dominated by the bulk properties, the surface layers have little effect on the linear wave propagation. As far as nonlinear optical effects are concerned, we can assume that the surface layer have the same linear refractive indices as the adjoining bulk media, but their nonlinear optical susceptibilities are different from the bulk. Unlike the linear case, the surface layer can strongly affect the nonlinear optical output in some cases.’

The insight in these words is the basis for the later treatment by Shen to substitute the macroscopic dielectric constant of the interface layer in the early treatment^{34,54} with the microscopic local field factors.^{41,53,56} This implies that the linear macroscopic dielectric constant of the interface layer does not need to be considered. Here the rigorous molecular optics treatment in the Section II and III with the discrete induced dipole lattice model is providing a further support for this approach.

Based on the following reasonings, the linear macroscopic dielectric constant of the monolayer or submonolayer is not an issue in the molecular optics approach described in the Section II and III explicitly.

a. Firstly, we consider a few nonlinear induced dipoles situated at the interface between the two isotropic bulk phases, for example, the vacuum/metal or other fluid/solid interfaces. These interface induced dipoles are situated in the vacuum phase and they does not even form an interface layer. Therefore, under the submonolayer condition up to a full monolayer condition, the treatment as presented in the Section II and III with the discrete induced dipole lattice model is rigorous, and no linear macroscopic dielectric constant can be invoked for the molecular layer. When this is validated, then consider the case that there is a submonolayer up to a full monolayer on top of the first full monolayer at the air/metal interface. The treatment of this top layer must be the same, i.e., no need to invoke a linear macroscopic dielectric constant for this top layer, and only the microscopic local field effect, i.e. the dipole screening effect, need to be considered.^{56,88} Since the interface layer in between any two isotropic bulk phases is usually one or few molecular monolayer thick, the discrete induced dipole lattice model must be a generally realistic treatment of the interface problem. In simple words, this implies that there is no such thing can be defined as the linear macroscopic dielectric constant for the interface layer.

b. Secondly, let us consider the case for the submonolayer adsorption of organic molecules at the air/liquid, e.g. submonolayer of surfactant molecules at the air/water interface. Since the air/water interface is known as sharp as less than 4\AA ,^{99,100,101} one can surmise that the hydrophobic part is in the air phase and the hydrophilic part is in the water phase. In this case, the treatment in the Section II and III with discrete induced dipole lattice model is generally a realistic treatment of the interface problem, especially for the SFG-VS when the tail and the head group of the interfacial surfactant molecule are probed with different vibrational frequencies. The radiation from the molecular induced dipole in the phase 2 (ε_2) can also be treated similarly and readily as in the Section II and III. Nevertheless, in these cases, the continuous surface sheet layer model does not provide a realistic representation of the microscopic molecular picture.

In the above cases, the linear macroscopic dielectric constant of the interface layer should not be a concern for the surface nonlinear optics whenever the surface contribution is dominant. Therefore, the macroscopic optical field at the interface can be well described with an explicit two phase model, as in the Eq.36. The major concern by Roy⁵⁷ on the macroscopic linear anisotropy of the interface monolayer in the SHG treatment is not a real issue at least for the submonolayer up to the monolayer regime.²⁶ Nevertheless, according to the treatment presented in the Section II and III, the local field effects of the induced dipoles at the interfaces need to be properly treated. This separation

of the macroscopic and the microscopic anisotropy of the interfacial monolayer is the ensurance of the simplicity and effectiveness in interpretation of the surface SHG and SFG-VS data.

Of course, above discussion may not be fully suitable for the situation when the interface consists of a big number of layers of the anisotropic nonlinear induced dipoles. However, as long as such film is thin enough not to significantly alter the macroscopic reflection and transmission coefficients of light from the interface between the two isotropic phases, there is no reason that one should worry about the issue of the linear macroscopic dielectric constant of the film itself.^{26,57}

B. The planewise dipole sum rule and the local field factor in the interface layer

The treatment of the microscopic local field effect as expressed in the Eq.13 in the Section II is similar to the results as Ye and Shen's earlier work.⁵⁶ The only difference is that now the general contribution from layers other than the interface monolayer is now included. To implement these formulae to correctly calculate or estimate the local field factors, the planewise dipole sum rule in the molecular crystal dielectric theory need to be invoked.^{73,74,75,76,77,78} The implementation of the planewise dipole sum rule in studying the interface problem was discussed by Munn *et al.* in the 1990s.^{49,79,80,81,82} However, its implication has not been picked up by others in the SHG and SFG-VS community so far. These issues needs to be addressed.

Now let us look at the actual problems in the interpretation of the SHG measurement data. In their SHG studies of the self-assembled-monolayer (SAM) at the gold substrate, Eisert *et al.* carefully compared the results with the macroscopic three layer model and the two layer model, as well as the local field corrections. They concluded that using the two-layer model without local-field correction gave most satisfactory agreement of the molecular orientation with the results from the NEXAFS and IR spectroscopy measurements.⁵¹ According to Eisert *et al.*, the parameters used to calculate the local field factors in the Eq.13 and the Eq.14 of the pNA [O₂N-C₆H₄-] monolayer in the SHG experiment are: $a = 5$ to 5.5\AA , $\alpha_{aa} = \alpha_{bb} = 16.4\text{\AA}^3$, $\alpha_{cc} = 27.3\text{\AA}^3$, and $\theta \sim 52^\circ$ from NEXAFS measurement. Then, one has $\alpha_{xx} = \alpha_{yy} = 19.8\text{\AA}^3$ and $\alpha_{zz} = 20.5\text{\AA}^3$, then $l_{xx} = l_{yy} = 3.51$ to 2.16 and $l_{zz} = 0.403$ to 0.473 . Therefore, the effective microscopic dielectric constant defined as $\varepsilon' = n'^2 = l_{yy}/l_{zz}$ becomes 8.71 to 4.57 , or $n' = 2.95$ to 2.14 . Here the definition $\varepsilon' = n'^2 = l_{xx}/l_{zz}$ follows the definition by Wei *et al.*⁴¹ These are unreasonably large values and the calculation by Eisert *et al.* concluded that in order to get the $\theta \sim 52^\circ$ from the SHG data, n' has to be close to unity, i.e. neglecting the microscopic local field effect.

Such conclusion by Eisert *et al.* is in direct disagreement with the formulation provided by Shen *et al.*⁴¹ However, the formulation with the microscopic local field factors by Shen *et al.* is validated by the treatment in this work. The answer to Eisert *et al.*'s difficulties in calculating the local field factors lies in the planewise dipole sum rule,^{73,74,75,76,77,78} which Munn *et al.* used to tackle the problem of overestimation of the local field factors by putting the linear polarizability of the whole molecule into the Eq.13.^{49,79,80,81,82}

The planewise dipole sum rule was originally developed in explaining optical and dielectric phenomena in molecular crystals, such as the long range coupling of the exciton in the molecular crystal, in the early 1970s.^{73,74,75,76,77,78} It has been known that the plane sum in the summation of the dipole-dipole interaction as in the Eq.6, which leads to expressions of the local field factors in the Eq.13, falls off exponentially as the perpendicular distance from the plane of the origin increases.^{76,77} Philpott *et al.* showed that even for the strong dipoles in the molecular crystals, the contribution of the immediate neighboring layer is only less than 1% of the contribution of the plane of the origin, and the total sum of all the rest of the layers up to infinity distance other than the plan of origin is generally less than 10%.^{76,77}

Based on this planewise dipole sum rule, when the lateral distance between the molecules is smaller than the length of the molecule, there is no reason to view the molecule as a whole when calculating the local field factors using the Eq.13. Munn *et al.* thus proposed a bead model to divide the long chain into a chain of sphere beads in calculating the local field factor for each submolecular segment layer for the long chain molecules in the Langmuir-Blodgett film.^{49,79,80,81,82} This bead model is also unknowingly supported by the calculations by Ye and Shen on the contribution of the local field factors from the image induced dipoles at a vacuum/metal interface.⁵⁶ They conclude that for $\varepsilon_{\text{metal}} = 10$, i.e. $(\varepsilon - 1)/(\varepsilon + 1) \sim 1$, when $d/a > 1/2$, the image induced dipole contribution is negligible. Here $d/a > 1/2$ is just the sphere bead condition in Munn's treatment if the interfacial induced dipole and its image induced dipole are considered as a whole unit.

In our treatment, the planewise dipole sum rule is explicitly described with the Eq.10. Evaluation of the ξ_0^l term indicates that in most of the cases, even the immediate neighboring term, i.e. $l = \pm 1$, is often negligible when d is larger than 3\AA . This indicates that when dealing with the local field factor calculations with the Eq.13, the depth of the segmentation of the molecular layer is generally not more than 3\AA . However, this number may not be correct for the big chromophores with conjugate structures, which may require quantum mechanical treatment or more complex models rather than the simple classical dipole model.

With the planewise dipole sum rule in mind, now one can understand why in the Eisert *et al.* case⁵¹ that the local field factors are over estimated than the actual value. Because the SAM monolayer is closely packed, if one use the α_{ii} value of the whole pNA group, the l_{ii} factors should be more deviated from the unity value. If one use the sphere

bead model, the l_{ii} is going to be much more close to unity. Actually, if closely inspect the formulae in the Eq.13, one can expect that when $|\alpha_{ii}\xi_0/2a^3| > 1$, the l_{xx} and l_{yy} can even become a large negative value. If the sphere bead model is not used, a closely packed long chain molecular monolayer would easily have unreasonable local field factors according to the Eq.13 without considering the planewise sum rule. Therefore, the planewise dipole sum rule is very important and has to be implemented for the evaluation of the microscopic local field factors in the molecular monolayer.

One direct conclusion from the segmentation of the interfacial molecules for the implementation of this planewise dipole sum rule is that because the different groups in the same molecule has different linear polarizabilities, and because the same molecular group may have different polarizabilities at different frequencies, their local field factors can be significantly different when these groups occupies different segmented layers when the monolayer is closely packed. This immediately poses questions to the practice of using the same and simple value for the interface local field factors in the SHG and SFG-VS studies.^{53,58,68} One of the example is for the SHG and SFG-VS studies of the 5CT [$\text{CH}_3-(\text{CH}_2)_4-(\text{C}_6\text{H}_4)_3-\text{CN}$] monolayer at the air/water interface.⁵³ In the interpretation of the SHG measurement of the $-(\text{C}_6\text{H}_4)_3-\text{CN}$ chromophore and the SFG-VS measurement of the $-\text{CH}_3$ and $-\text{CN}$ groups of the 5CT monolayer, the same local field factor value, i.e. $n' = 1.18$, was used for all three molecular chromophore or groups. Close inspection shows that the orientational angle thus obtained is actually inconsistent with other studies.^{102,103,105,106} Therefore, whether the same $n' = 1.18$ value is suitable for the three groups needs to be re-examined. In a recent study in our research group, using a self-consistent approach we found that the $n'(800\text{nm}) \sim 1.5$ and $n'(400\text{nm}) \sim 2.5$ for the $-(\text{C}_6\text{H}_4)_3-\text{CN}$ chromophore from the SHG data, significantly different from that of the $-\text{CH}_3$ or $-\text{CN}$ group, and consistent with the large polarizability of the $-(\text{C}_6\text{H}_4)_3-\text{CN}$ chromophore.^{104,105} The orientational angle thus obtained for the $-(\text{C}_6\text{H}_4)_3-\text{CN}$ chromophore in the closely packed Langmuir monolayer at the air/water interface is about 20° , consistent with the orientational angle obtained in other studies.^{102,103}

Now, if the ϵ' or n' values should be different, why in the past SFG-VS studies it was quite successful to use the simple values such as $n' = 1.18$, or the average value of the optical constant of the two neighboring bulk phases for molecular groups and chromophores at the common dielectric interfaces?^{21,25,53,58,68,106} Here we can show that these values are actually quite reasonable approximation of the common simple molecular groups such as $-\text{CH}_3$, $-\text{C}=\text{O}$, etc. at the interface.

The experimental linear polarizability values of many common molecular group are as listed in the Table I.^{93,94,95} The values for simple organic groups are typically in the range of 1.5 to 3.0 \AA^3 . Considering that the segmentation depth is expected to be not more than 3\AA for simple molecules with no big chromophores with conjugated structure, as a realistic approximation, the typical α value used in the calculation is set in between 2 to 4 \AA^3 . Considering the fact that at the molecular interface a typical molecular group per area is about 20 \AA^2 (square lattice constant $a \sim 4.5\text{\AA}$) to 30 \AA^2 ($a \sim 5.5\text{\AA}$), simulations in Table II shown that the typical ϵ' value for these groups are 1.17 - 1.56 , i.e. $n'=1.08$ - 1.32 , depending on the lattice constant and the value of the polarizability.

In above calculation we assumed that the monolayer is closely packed. If the interfacial monolayer is sparse, the local field effect shall be small. For the situation of submonolayer adsorption at the liquid-liquid interface, then the dipole interactions of the solvent molecules in the interface plane need to be considered.

These values are generally in between the vacuum and the substrate dielectric constant, as used in the literature. They are also close to the estimation made by Zhuang *et al.* using a modified Lorentz model of the interface,⁵³ and the simple average of the optical constant of the two adjacent isotropic bulk phases.^{52,58,68} However, even though these values worked almost fine, the models and the reasonings behind it prevented the treatment of the molecular details of the molecular interface. With the development of the laser techniques and the measurement methodology in the surface SHG and SFG-VS,^{21,25,39,40} now such details can be interrogated from the careful experiments. This shall provide new opportunities for the interface studies.

TABLE I: Experimental polarizabilities values for common molecular groups from the literatures.⁹⁴

group	$\alpha(\text{\AA}^3)$	group	$\alpha(\text{\AA}^3)$
$-\text{COOH}$	2.86	$-\text{SH}$	3.47
$-\text{CH}_3$	2.24	$-\text{CN}$	2.16
$-\text{CH}_2-$	1.84	$-\text{NH}_2$	1.76
$-\text{C}=\text{O}$	1.82	H_2O	1.45

Of course the above simple estimation does not include the bigger chromophore, such as phenyl, and biphenyl etc. Their polarizability is generally much larger, and the local field effects can be much stronger when they are closely aligned at the interface. According to the Eq.13, it is possible to have the $l_{xx} = l_{yy}$ to be smaller than unity or even go to negative values, and l_{zz} to be larger than unity, when the molecules with relatively larger linear polarizability are closely packed even far from resonance. These are the unique phenomena for the two dimensional anisotropic

TABLE II: Simulation of local field factors ε' and n' with the α value between 2 and 4 \AA^3 . The case for $\alpha = 1.5\text{\AA}^3$ is the simulation results of the interfacial water molecules.

$\alpha(\text{\AA}^3)$	$a(\text{\AA})$	$l_{xx} = l_{yy}$	l_{zz}	ε'	n'
2.0	4.5	1.11	0.84	1.33	1.15
2.0	5.5	1.06	0.90	1.17	1.08
4.0	4.5	1.25	0.72	1.74	1.32
4.0	5.5	1.12	0.82	1.37	1.17
1.5	3.5	1.19	0.76	1.56	1.25
1.5	4.0	1.12	0.83	1.36	1.16

local field factors. According to the Lorentz relation, this is not possible for the optical bulk materials with normal dispersion. Such phenomena are certainly yet to be explored experimentally.

The local field factors in the molecular layer is dependent on the orientation and also on how the segmentation is done, and one generally does not have the detailed knowledge of these information beforehand. Therefore, different approximation approaches were employed in the past SHG and SFG-VS studies. Similar to what Munn *et al.* did previously,^{49,79,80,81,82} we invoked the planewise dipole sum rule here to show that in calculating the local field factors using the microscopic point dipole model using formulae in the Eq.13, extreme care must be taken in order not to overestimate the local field effects. However, this does not imply that the sphere bead model always generates more reasonable results for the local field factors. We want to point out that when the square lattice constant is close to or even smaller than the size of the molecule under studying, the simple point dipole model is expect to breakdown, and the planewise dipole sum rule can be used as the remedy to some extent. One expects that there is no simple rule to segment the chain molecules in calculating the local field factors. Down to the detailed molecular level, quantum mechanic treatment of the electron density and their polarizability should be employed to make more accurate description of the molecules at the interface. Nevertheless, the above estimation can give the reasonable upper and lower bound of the local field factors.

C. SHG or SFG-VS experiments to test the microscopic model

Here we discuss how SHG and SFG-VS experiment can be used to test the microscopic model.

The key point raised in this study is that the molecular optics treatment of the interface nonlinear radiation can provide a detailed microscopic description of the nonlinear optical processes and the molecular behaviors at the interface. The key to test the microscopic model is to find way to determine the microscopic local field factors or to quantitatively determine their effects in the SHG or SFG-VS experiment, and to compare these experimental effects with the molecular details in the molecular monolayer.

There were few attempts trying to experimentally determine the interfacial effective optical constants with SHG^{58,68} and SFG-VS.⁶⁷ All of them concluded for a value close to the simple arithmetic average of the optical constant of the two adjacent bulk phases. These works were not based on the microscopic model and they can not be used to test the microscopic model. Because the microscopic model predicts that the local field factors, which is connected to the effective optical constant of the interface layer through the relationship $\varepsilon' = n'^2 = l_{yy}/l_{zz}$,^{41,53} must depend on the detailed structure of the molecular monolayer and may have values other than the simple arithmetic average or the prediction with the modified macroscopic Lorentz model of the interface.⁵³

The first test is to determine the local field factor l_{yy}/l_{zz} for the closely packed Langmuir monolayers at the air/water interface with large chromophores. According to the Eq.13, when $\alpha_{ii} \sim 15\text{\AA}^3$ and $a^2 \sim 40\text{\AA}^2$, one has that $\varepsilon' = l_{yy}/l_{zz} \sim 2.10$, thus $n' \sim 1.45$. These kind of conditions can be easily satisfied with chromophore with two or three phenyl groups, such as the alkyl cyano-biphenyl (nCB) or the alkyl cyano-triphenyl (nCT) Langmuir films. It has been shown that in the closely packed 8CB Langmuir monolayer at the air/water interface, since the molecular surface density is always known, a self-consistent analysis of the polarization dependent SHG data at different surface density can give the molecular orientation angle and the ε' value at different surface densities.^{37,105} Such self-consistent analysis was suggested by Munn *et al.* before, because they realized that the determination of the molecular orientational angle and the determination of the interface local field factor are interconnected.⁸⁰ Such self-consistent analysis can only be carried out for the Langmuir or Langmuir-Blodgett monolayers because their surface density are known and can be varied controllably. It turned out in our SHG studies that for the 8CB monolayer, the ε' changes from 1.7 to 2.4 when the surface density changes from 51\AA^2 to 39\AA^2 per molecule.^{104,105} These results agree very well with the Eq.13, and the orientational angle thus obtained agree well with the rod model of the chromophore. This is a very convincing example to show that the local field factors of the molecular monolayer do not have simple

values close to the arithmetic average of the two adjacent bulk phases. The detail of this study is to be published elsewhere.^{104,105}

Another test can be designed with the SFG-VS measurement of the small rigid linear molecules, such as the acetonitrile molecule, at the air/liquid interface. For example, SFG-VS can selectively measure polarization dependent vibrational spectra of both the $-CH_3$ and the $-CN$ groups of the interface acetonitrile molecule.¹⁰⁷ Since the molecule is linear, the orientation angles, which are dependent on the values of ϵ'_{-CN} and ϵ'_{-CH_3} respectively, determined from the $-CH_3$ and the $-CN$ SFG-VS data should give the same value. Thus the ratio $\epsilon'_{-CN}/\epsilon'_{-CH_3}$ can be determined experimentally. Using the polarization null angle method in SFG-VS,^{21,108,109,110} the ratio of the local field factor for the $-CH_3$ and the $-CN$ groups, i.e. $\epsilon'_{-CN}/\epsilon'_{-CH_3}$, can be obtained quite accurately. This value is indeed different from unity and it is beyond the experimental error bar. This observation can not be explained by the previous models, but can be well explained and quantitatively analyzed with the microscopic model in this work. The detail of the experimental study and analysis is going to be reported elsewhere.¹¹¹

More SHG or SFG-VS experiments can be designed accordingly to test the microscopic model. Detail analysis of SHG and SFG-VS data is now possible with the recent development of quantitative polarization measurement in SHG and SFG-VS.^{21,25,112,113} These studies not only can provide test for the microscopic model, but also can provide detailed information of the molecular interface according to the microscopic model.

V. CONCLUSION

Because the SHG and the SFG-VS have been proven as the sensitive probes for interfaces with the submonolayer coverage,^{2,4,8,10} the treatment based on the more realistic discrete induced dipole lattice model is developed in this report. Recent development in quantitative polarization and symmetry analysis in SHG and SFG-VS have provided new opportunities in the interface studies.^{21,25} These development also provided more accurate data to test the SHG and SFG-VS theories at the detailed molecular level.^{37,39,40,53,58}

In this report we have taken the molecular optics theory approach and treated the molecular interface with more realistic discrete induced dipole lattice model. Based on this model, the following results are derived: a. the detailed expressions of the local field factors in the interface molecular layer; b. the detailed expressions for the far field radiation of the SHG as well as the SFG-VS process from the interface induced dipoles. It turned out that the asymptotic results for the far field radiation is in the same form as the results derived from the famous infinitesimally thin polarization sheet layer by Heinz and Shen using the Maxwell equation with the boundary conditions,^{4,54} as well as their later modifications with the consideration of the microscopic local field factors using the classical dipole model.^{41,53,56} This not only validates the effectiveness of the original formulation from the works by Shen and colleagues, but also validates the success of the molecular optics theory approach developed here.

According to Born and Wolf, the molecular optics theory can directly connect the macroscopic optical phenomena to the molecular properties, and can provide deeper physical insight into electromagnetic interaction problems than does the rather formal approach based on Maxwell's phenomenological equations.^{83,84} Based on the microscopic and discrete induced dipole lattice model, the problem of the macroscopic dielectric constants of the interfacial molecular monolayer is discussed and clarified. We explicitly demonstrated that the macroscopic dielectric constant of the molecular submonolayer and monolayer does not need to be invoked in the microscopic model of the surface nonlinear optics. Based on the planewise dipole sum rule and the previous work by Munn *et al.*, the issue on how the microscopic local field factors are evaluated was discussed. According to these results, the effectiveness and limit of the simple models on the effective dielectric constant of the interfacial molecular monolayer are discussed and evaluated. However, for simple and small molecular groups, the simple models does provide good approximation of the microscopic local field effects of the interfacial molecular monolayer. SHG and SFG-VS experimental tests of the microscopic discrete induced dipole lattice model are also discussed. With these developments, many previous SHG and SFG-VS studies are better understood and evaluated. Moreover, these developments can provide a full microscopic description of the nonlinear radiation from the molecular interface. Detailed molecular information can be obtained from the model developed in this work, together with better and more accurate polarization measurement data in SHG and SFG-VS.

The microscopic molecular optics approach can also be applied to the treatment of the ellipsometry response from the molecular monolayer interface. When ellipsometry is to be applied to study such interfaces, a microscopic molecular theory for the ellipsometry is certainly needed. So far, the treatment on the ellipsometry and the treatment of the SHG or SFG-VS are not fully consistent in description of the anisotropy in the molecular layer. We shall discuss these issues elsewhere.

In conclusion, aside from the macroscopic theory of the surface SHG and SFG-VS, an effective microscopic molecular optics theory is developed in this work. Such development may shed new light on both the linear and the nonlinear optics interface studies.

Acknowledgment. DSZ thanks the helpful discussion from Wen-kai Zhang, Yu-jie Sun and Yuan Guo. HFW thanks

the support by the Natural Science Foundation of China (NSFC, No.20373076, No.20425309, No.20533070).

-
- ¹ Y. R. Shen, *Ann. Rev. Mat. Sci.* **16**, 69 (1986).
 - ² Y. R. Shen, *Nature* **337**, 519 (1989).
 - ³ G. L. Richmond, J. M. Robinson and V. L. Shannon, *Prog. Surf. Sci.* **28**, 1 (1988).
 - ⁴ Y. R. Shen, *Annu. Rev. Phys. Chem.* **40**, 327 (1989).
 - ⁵ V. Vogel, and Y. R. Shen, *Annu. Rev. Mat. Sci.* **21**, 515 (1991).
 - ⁶ K. B. Eisenthal, *Annu. Rev. Phys. Chem.* **43**, 627 (1992).
 - ⁷ K. B. Eisenthal, *Acc. Chem. Res.* **26**, 636 (1993).
 - ⁸ R. M. Corn and D. A. Higgins, *Chem. Rev.* **94**, 107 (1994).
 - ⁹ C. D. Bain, *J. Chem. Soc. Faraday Trans.* **91**, 1281 (1995).
 - ¹⁰ K. B. Eisenthal, *Chem. Rev.*, **96**, 1343 (1996).
 - ¹¹ P. B. Miranda, and Y. R. Shen, *J. Phys. Chem. B* **103**, 3292 (1999).
 - ¹² G. A. Somorjai, and G. Rupprechter, *J. Phys. Chem. B* **103**, 1623 (1999).
 - ¹³ M. J. Shultz, C. Schnitzer, D. Simonelli, and S. Baldelli, *Int. Rev. Phys. Chem.* **19**, 123 (2000).
 - ¹⁴ Y. R. Shen, *IEEE J. Sel. Top. Quant. Elec.* **6**, 1375 (2000).
 - ¹⁵ G. L. Richmond, *Annu. Rev. Phys. Chem.* **52**, 357 (2001).
 - ¹⁶ M. Buck, and M. Himmelhaus, *J. Vac. Sci. Tech. A* **19**, 2717 (2001).
 - ¹⁷ Y. R. Shen, *Pure Appl. Chem.* **73**, 1589 (2001).
 - ¹⁸ G. L. Richmond, *Chem. Rev.* **102**, 2693 (2002).
 - ¹⁹ Z. Chen, Y. R. Shen, and G. A. Somorjai, *Annu. Rev. Phys. Chem.* **53**, 437 (2002).
 - ²⁰ F. Vidal, and A. Tadjeddine, *Rep. Prog. Phys.* **68**, 1095 (2005).
 - ²¹ H. F. Wang, W. Gan, R. Lu, Y. Rao, and B. H. Wu, *Int. Rev. Phys. Chem.*, **24**, 191 (2005).
 - ²² Y. R. Shen, and V. Ostroverkhov, *Chem. Rev.* **106**, 1140 (2006).
 - ²³ S. Gopalakrishnan, D. F. Liu, H. C. Allen, M. Kuo, and M. J. Shultz, *Chem. Rev.* **106**, 1155 (2006)
 - ²⁴ K. B. Eisenthal, *Chem. Rev.* **106**, 1462 (2006).
 - ²⁵ W. K. Zhang, H. F. Wang, and D. S. Zheng, *Phys. Chem. Chem. Phys.* **8**, 4041 (2006).
 - ²⁶ Y. R. Shen, *The Principles of Nonlinear Optics* (Wiley, New York, 2003). Chapter 25.
 - ²⁷ C. K. Chen, A. R. B. Decastro, and Y. R. Shen, *Phys. Rev. Lett.* **46**, 145 (1981).
 - ²⁸ T. F. Heinz, C. K. Chen, D. Ricard, Y. R. Shen, *Phys. Rev. Lett.* **48**, 478 (1982).
 - ²⁹ T. F. Heinz, H. W. K. Tom, and Y. R. Shen, *Phys. Rev. A* **28**, 1883 (1983).
 - ³⁰ Y. R. Shen, *J. Vac. Sci. Tech. B* **3**, 1464 (1985).
 - ³¹ P. Guyot-sionnest, W. Chen, and Y. R. Shen, *Phys. Rev. B* **33**, 8254 (1986).

- ³² X. D. Zhu, H. Suhr, and Y. R. Shen, *Phys. Rev. B* **35**, 3047 (1987).
- ³³ P. Guyot-Sionnest, R. Superfine, J. H. Hunt, and Y. R. Shen, *Chem. Phys. Lett.* **144**, 1 (1988).
- ³⁴ M. B. Feller, W. Chen, and Y. R. Shen, *Phys. Rev. A* **43**, 6778 (1991).
- ³⁵ N. Bloembergen, and P. S. Pershan, *Phys. Rev.* **128**, 606 (1962).
- ³⁶ G. J. Simpson, and K. L. Rowlen, *Acc. Chem. Res.* **33**, 781 (2000).
- ³⁷ Y. Rao, Y. S. Tao, and H. F. Wang, *J. Chem. Phys.* **119**, 5226 (2003).
- ³⁸ W. Gan, D. Wu, Z. Zhang, R. R. Feng, and H. F. Wang, *J. Chem. Phys.* **124**, 114705 (2006).
- ³⁹ W. Gan, B. H. Wu, Z. Zhang, Y. Guo, and H. F. Wang, *J. Phys. Chem. C* **111**, 8716 (2007).
- ⁴⁰ W. Gan, Z. Zhang, R. R. Feng, and H. F. Wang, *J. Phys. Chem. C* **111**, 8726 (2007).
- ⁴¹ X. Wei, S. C. Hong, X. W. Zhuang, T. Goto, and Y. R. Shen, *Phys. Rev. E* **62**, 5160 (2000).
- ⁴² T. G. Zhang, C. H. Zhang, and G. K. Wong, *J. Opt. Soc. Am. B* **7**, 902 (1990).
- ⁴³ L. M. Hayden, *Phys. Rev. B* **38**, 3718 (1988).
- ⁴⁴ J. F. McGilp, Z. R. Tang, and M. Cavanagh, *Syn. Met.* **61**, 181 (1993).
- ⁴⁵ G. Cnossen, K. E. Drabe, D. A. Wiersma, M. A. Schoondorp, A. J. Schouten, J. B. E. Hulshof, and B. L. Feringa, *Langmuir* **9**, 1974 (1993).
- ⁴⁶ Z. R. Tang, M. Cavanagh, and J. F. McGilp, *J. Phys.: Cond. Matt.* **5**, 3791 (1993).
- ⁴⁷ G. Cnossen, K. E. Drabe, and D. A. Wiersma, *J. Chem. Phys.* **97**, 4512 (1992).
- ⁴⁸ H. Ui, A. Tomioka, T. Nishiwaki, and K. Miyano, *J. Chem. Phys.* **101**, 6430 (1994).
- ⁴⁹ R. W. Munn, and M. M. Shabat, *J. Chem. Phys.* **99**, 10059 (1993).
- ⁵⁰ E. Mishina, Y. Miyakita, Q. K. Yu, S. Nakabayashi, and H. Sakaguchi, *J. Chem. Phys.* **117**, 4016 (2002).
- ⁵¹ F. Eisert, O. Dannenberger, and M. Buck, *Phys. Rev. B* **58**, 10860 (1998).
- ⁵² J. A. Ekhoﬀ, and K. L. Rowlen, *Anal. Chem.* **74**, 5954 (2002).
- ⁵³ X. Zhuang, P. B. Miranda, D. Kim, and Y. R. Shen, *Phys. Rev. B* **59**, 12632 (1999).
- ⁵⁴ T. F. Heinz, *Ph.D Dissertation*, Univeristy of California, Berkeley (1982).
- ⁵⁵ T. F. Heinz, *Nonlinear Optical Effects at Surfaces and Interfaces*, in *Nonlinear Surface Electromagnetic Phenomena*, ed. by H. E. Ponath and G. I. Stegman (North-Holland, Armsterdam, 1991), pp. 353-416.
- ⁵⁶ P. X. Ye, and Y. R. Shen, *Phys. Rev. B* **28**, 4288 (1983).
- ⁵⁷ D. Roy, *Phys. Rev. B* **61**, 13283 (2000).
- ⁵⁸ G. J. Simpson, C. A. Dailey, R. M. Plocinik, A. J. Moad, M. A. Polizzi, and R. M. Everly, *Anal. Chem.* **77**, 215 (2005).
- ⁵⁹ R. M. A. Azzam, and N. M. Bashara, *Ellipsometry and Polarized Light* (Elsevier, Amsterdam, 1987).
- ⁶⁰ O. S. Heavens, *Optical Properties of Thin Solid Films* (Dover Publications, Inc., New York, 1991).
- ⁶¹ P. Guyot-sionnest, Y. R. Shen, and T. F. Heinz, *Appl. Phys. B* **42**, 237 (1987).
- ⁶² N. Bloembergen, *Nonlinear Optics* (Benjamin, New York, 1965). p69.
- ⁶³ D. Lupo, W. Prass, U. Scheunemann, A. Laschewsky, H. Ringsdorf, and I. Ledoux, *J. Opt. Soc. Am. B* **5**, 300 (1988).

- ⁶⁴ H. Hsiung, G. R. Meredith, H. Vanherzeele, R. Popovitzbiro, E. Shavit, and M. Lahav, *Chem. Phys. Lett.* **164**, 539 (1989).
- ⁶⁵ J. E. Sipe, *J. Opt. Soc. Am. B* **4**, 481 (1987).
- ⁶⁶ V. Mizrahi, and J. E. Sipe, *J. Opt. Soc. Am. B* **15**, 660 (1988).
- ⁶⁷ J. Wang, Z. Paszti, M. A. Even, and Z. Chen, *J. Phys. Chem. B* **108**, 3625 (2004).
- ⁶⁸ J. G. Frey, *Chem. Phys. Lett.* **323**, 454 (2000).
- ⁶⁹ R. R. Naujok, H. J. Paul, and R. M. Corn, *J. Phys. Chem.* **100**, 10497 (1996).
- ⁷⁰ D. A. Higgins, M. B. Abrams, S. K. Byerly, and R. M. Corn, *Langmuir* **8**, 1994 (1992).
- ⁷¹ R. Braun, B. D. Casson, and C. D. Bain, *Chem. Phys. Lett.* **245**, 326 (1995).
- ⁷² R. W. Munn, *J. Chem. Phys.* **103**, 850 (1995).
- ⁷³ F. W. Wette, and G. E. Schacher, *Phys. Rev.* **137**, A78 (1965).
- ⁷⁴ C. D. Mahan, and G. Obermair, *Phys. Rev.* **183**, 834 (1969).
- ⁷⁵ M. R. Philpott, *J. Chem. Phys.* **56**, 996 (1972).
- ⁷⁶ M. R. Philpott, *J. Chem. Phys.* **58**, 598 (1972).
- ⁷⁷ M. R. Philpott, and J. W. Lee, *J. Chem. Phys.* **58**, 595 (1973).
- ⁷⁸ M. R. Philpott, *J. Chem. Phys.* **61**, 5306 (1974).
- ⁷⁹ M. I. H. Panhuis, and R. W. Munn, *J. Chem. Phys.* **112**, 6763 (2000).
- ⁸⁰ M. I. H. Panhuis, and R. W. Munn, *J. Chem. Phys.* **112**, 10691 (2000).
- ⁸¹ M. I. H. Panhuis, and R. W. Munn, *J. Chem. Phys.* **112**, 10685 (2000).
- ⁸² R. W. Munn, and M. M. Shabat, *J. Chem. Phys.* **99**, 10052 (1993).
- ⁸³ E. Lalor, and E. Wolf, *J. Opt. Soc. Am.* **62**, 1165 (1972).
- ⁸⁴ M. Born, and E. Wolf, *Principles of Optics: Electromagnetic Theory of Propagation, Interference and Diffraction of Light (6th Edition)*, Cambrige Unverisity Press, p38-41, p81-84, p104-108 (1997).
- ⁸⁵ A. V. Ghiner, and G. I. Surdutovich, *Phys. Rev. A* **49**, 1313 (1994).
- ⁸⁶ J. A. Armstrong, N. Bloembergen, J. Ducuing, and P. S. Pershan, *Phys. Rev.* **127**, 1918 (1962).
- ⁸⁷ N. Bloembergen, *IEEE J. Sel. Top. Quant. Electron.* **6**, 876 (2000).
- ⁸⁸ A. Bagchi, R. G. Barrera, and B. B. Dasgupta, *Phys. Rev. Lett.* **44**, 1475 (1980).
- ⁸⁹ A. Bagchi, R. G. Barrera, and R. Fuchs, *Phys. Rev. B* **25**, 7086 (1982).
- ⁹⁰ M. Iwamoto, Y. Mizutani, and A. Sugimura, *Phys. Rev. B* **54**, 8186 (1996).
- ⁹¹ J. Topping, *Proc. R. Soc. London, A* **114**, 67 (1927).
- ⁹² C. Hirose, N. Akamatsu, and K. Domen, *Appl. Spec.* **46**, 1051 (1992).
- ⁹³ K. J. Miller, and J. A. Savchik, *J. Am. Chem. Soc.* **101**, 7206 (1979).
- ⁹⁴ K. J. Miller, *J. Am. Chem. Soc.* **112**, 8533 (1990).
- ⁹⁵ K. J. Miller, *J. Am. Chem. Soc.* **112**, 8543 (1990).
- ⁹⁶ R. W. Boyd, *Nonlinear Optics* (Academic Press, Inc., New York, 1992). p65.

- ⁹⁷ P. F. Brevet, *Surface Second Harmonic Generation* (Press Polytechniques et Universitaires Romandes, Lausanne, 1997).
- ⁹⁸ W. K. Zhang, D. S. Zheng, Y. Y. Xu, H. T. Bian, Y. Guo and H. F. Wang, *J. Chem. Phys.* **123**, 224713 (2005).
- ⁹⁹ R. M. Townsend, and S. A. Rice, *J. Chem. Phys.* **94**, 2207 (1991).
- ¹⁰⁰ A. Braslau, M. Deutsch, P. S. Pershan, A. H. Weiss, J. Als-Nielsen, and J. Bohr, *Phys. Rev. Lett.* **54**, 114 (1985).
- ¹⁰¹ A. Braslau, P. S. Pershan, G. Swislow, B. M. Ocko, and J. Als-Nielsen, *Phys. Rev. A* **38**, 2457 (1988).
- ¹⁰² A. Biadasz, T. Martyniski, R. Stolarski, and D. Bauman, *Liq. Crys.* **31**, 1639 (2004).
- ¹⁰³ R. Hertmanowski, T. Martyniski, and D. Bauman, *J. Mol. Struc.* **741**, 201 (2005).
- ¹⁰⁴ D. S. Zheng, *PhD Dissertation* (Institute of Chemistry, Chinese Academy of Sciences, Beijing, 2006).
- ¹⁰⁵ D. S. Zheng and H. F. Wang, unpublished work.
- ¹⁰⁶ J. Wang, C. Chen, S. M. Buck, and Z. Chen, *J. Phys. Chem. B* **105**, 12118 (2001).
- ¹⁰⁷ D. Zhang, J. H. Gutow, and K. B. Eisenthala, *J. Chem. Phys.* **98**, 5099 (1993).
- ¹⁰⁸ W. Gan, B. H. Wu, H. Chen, Y. Guo, and H. F. Wang, *Chem. Phys. Lett.* **406**, 467 (2005).
- ¹⁰⁹ R. Lu, W. Gan, and H. F. Wang, *Chin. Sci. Bull.*, 2003, **48**, 2183; R. Lu, W. Gan, and H. F. Wang, *Chin. Sci. Bull.*, 2004, **49**, 899.
- ¹¹⁰ H. Chen, W. Gan, B. H. Wu, D. Wu, Z. Zhang, and H. F. Wang, *Chem. Phys. Lett.*, 2005, **408**, 284.
- ¹¹¹ Z. Zhang and H. F. Wang, unpublished work.
- ¹¹² R. M. Plocinik, R. M. Everly, A. J. Moad, and G. J. Simpson, *Phys. Rev. B* **72**, 125409 (2005).
- ¹¹³ R. M. Plocinik, G. J. Simpson, *Anal. Chim. Acta* **496**, 133 (2003).